ABSTRACT

Microchannels are of current interest for use in compact heat exchangers, micro biochips, micro reactors, VLSI system where very high heat transfer performance is desired. These electronic equipments are virtually synonyms with modern life applications such as appliances, instruments and computers. The dissipation of heat is necessary for the proper functioning of these instruments Microchannels provide very high heat transfer coefficients because of their small hydraulic diameters. Here, an investigation of fluid flow and heat transfer in microchannels is conducted. Fluid flow and heat transfer experiments were conducted on a silicon microchannel heat exchanger (MHE) .A three-dimensional Computational Fluid Dynamics (CFD) model was built using the commercial package, FLUENT, to investigate the conjugate fluid flow and heat transfer phenomena in a silicon-based rectangular microchannel heat sink. This work focused on laminar flow (Re < 200) within rectangular microchannel with hydraulic diameter 86μm for single-phase liquid flow. The influence of the thermophysical properties of the fluid on the flow and heat transfer, are investigated by evaluating thermophysical properties at a reference bulk temperature.

The micro-heat sink model consists of a 10 mm long silicon substrate, with rectangular microchannels, 57μm wide and 180μm deep, fabricated along the entire length. water at 293K is taken as working fluid. The results indicate that thermophysical properties of the liquid can significantly Influence both the flow and heat transfer in the microchannel. Assumption of hydrodynamic, fully developed laminar flow is valid here on basis of Langhaar's equation. The local heat transfer coefficient and averaged Nusselt number is calculated and plotted for pressure drop of 50kpa, 30kpa and 10kpa.also result is verify for heat flux 50W/cm^2, 90W/cm^2 and 150 W/cm^2.

Table of Contents

Certificate

Acknowledgement

Abstract 1

Table of Contents 2

List of Figures 3

Nomenclature 6

1. Introduction 8

1.1 Introduction 10
1.2 New Thermal Design 13
1.3 Current Methods Used in Industry 14
1.3.1 Module Level Cooling 14
1.3.1.1 Internal Module Cooling 14
1.3.1.2 External Module Cooling 14
1.3.1.3 Immersion Cooling 14
1.3.2 System Level Cooling 15
1.3.2.1 Air Cooling 15
1.3.2.2 Hybrid Air-Water Cooling 16
1.3.2.3 Liquid-Cooling Systems 17
1.3.2.4 Refrigeration Cooled Systems 17
1.3.3 Data Center Thermal Management 18
1.4 Heat sink 20
1.5 Micro channel heat sink 20
1.5.1 Design parameters 20
1.5.2 Heat sink material 21

1.5.3 The number of fins 22

1.5.4 Fin shapes 23

1.5.5 Others parameters 23

1.5 Objective of the Work 24

1.6 Organization of the Thesis 25

2. Literature Review 26

2.1 Introduction 27

2.2 Micro channel concepts 28

2.3 Analytical studies 31

2.4Numerical studies 34

2.5 Experimental studies 38

2.6 Closure 42

3. Mathematical Formulation 43

3.1 Introduction 44

3.1.1 Description of the designed cooling model 45

3.1.2 Assumptions 46

3.2 governing equations 47

3.2.1 Continuity Equation 47

3.2.2 Momentum equation 47

3.2.3 Energy Equation 47

3.3 Boundary conditions 47

3.3.1 Hydraulic boundary conditions 47

3.3.2 Thermal boundary conditions 48

3.4 Background of theory 48

3.4.1Background of theory 48

3.4.2 Heat transfer by convection: 49

3.4.3Reynold`s Number 49
3.4.4 Nusselt Number 49
3.4.5 Prandtl number 50
3.4.6 Grashof number 50
3.4.7 Rayleigh number 50
3.4.8 Solution approaches 50
3.5 Computational fluid dynamics (cfd) & fluent 51
3.5.1 Finite volume method 51
3.5.2 Finite element method 52
3.5.3 Finite difference method 52
3.6 Schemes to calculate face value for variables 52
3.6.1 Central difference scheme 52
3.6.2 The upwind scheme 52
3.6.3 The exact solution 53
3.6.4 The exponential scheme 53
3.6.5 The hybrid scheme 53
3.7 Gambit and fluent steps 53
3.7.1 Gambit steps 55
3.7.2 Fluent steps 58
3.8 Closure 61

4. Results and Discussions 62
4.1 Introduction 64
4.2 Temperature contour 65
4.3 Velocity contour 72
4.4. Average heat transfer coefficient 73
4.5 Average Nusselt Number 75
4.6 Heat transfer coefficient variation for different heat flux 50,90 and 150W/cm^2 76
4.7 Nusselt number variation for different heat flux 77

4.8 Reynolds number verses Nusselt Number 78

4.9 Conclusion 82

4.10 Sources of Errors in CFD calculations 84

4.11 Closure 84

5. Bibliography 85

List of Figures

Figure No.	Title	Page No.
Fig. 1.1	Increase in circuit complexity	11
Fig. 1.2	The Chronological Evolution of chip level Heat Flux.	12
Fig. 1.3	Major Causes of Electronics Failure	12
Fig. 1.4	Cross Section of a Typical Module Denoting Internal Cooling Region and External Cooling Region	14
Fig 1.5	Heat load per product Footprint	19
Fig 1.6	Heat Sink Design Parameters	21
Fig 1.7	Thermal conductivities of common heat sink materials and Possible candidates	22
Fig 1.8	Cu MHE with channels molded, plenums cut, and holes drilled	23
Fig 1.9	Two Heat Sinks with different fin geometry	23
Fig 3.1	Geometric dimensions of single channel	46
Fig 3.2	Microchannel model: (a) side view; (b) model view.	57
Fig 4. 1	Local Temperature Distribution Temperature contour of Silicon material at X = 50μm for Δp=50 kpa and heat flux 90W/cm^2	64
Fig 4.2	Temperature contour of Silicon material at X = 50μm for Δp=50 kpa and heat flux 90W/cm^2 at outlet	65
Fig. 4.3	Temperature of Outlet at Adiabatic wall conditions for double parallel channel	65
Fig. 4.4	Temperature contour at Isothermal (300k) wall condition for parallel channel	66
Fig 4.5	Temperature contour of fluid at outlet for Pressure difference of 10kpa and heat flux of 90W/cm^2	67
Fig 4.6	Temperature contour of fluid at outlet for Pressure difference of 15kpa and heat flux of 90W/cm^2	68
Fig 4.7	Temperature contour of fluid at outlet for Pressure difference of 50kpa and heat flux of 90W/cm^2	68
Fig 4.8	Temperature contour of fluid at outlet for Pressure difference of 50kpa and heat flux of 50W/cm^2 at X=50μm	69
Fig 4.9	Temperature contour of fluid at outlet for Pressure difference of 50kpa and heat flux of 90W/cm^2	71

Fig 4.10 Temperature contour of fluid for pressure difference of 50kpa and heat flux of 150W/cm^2 72

Fig 4.11 Average temperature of liquid for different pressure drops and consant heat flux 90W/cm^2 at X=50 μm 73

Fig 4.12 Velocity contour of fluid at outlet for Pressure difference of 50kpa and heat flux of 150W/cm^2 74

Fig 4.13 Average heat transfer coefficient variation for pressure drop of 50kpa at $q"= 90\ W/cm^2$ at x = 50μm 75

Fig 4.14 Average heat transfer coefficient variation for different pressure drop(50kpa,15kpa,10kpa) at $q"= 90\ W/cm^2$ at x = 50μm 75

Fig4.15 Average Nusselt number variation for different pressure drop at $q"= 90\ W/cm^2$ at x = 50μm 77

Fig 4.16 Axial variation of average heat transfer coefficient for different heat fluxes at Δp = 50kpa 78

Fig 4.17 Axial variation of Nusselt number for different heat fluxes at Δp = 50kpa 79

Fig 4.18 Variation of Reynolds number vs. Nusselt number for different heat fluxes, at Δp = 50kpa at x = 50μm 80

Fig 4.19 Variation of Reynolds no vs Nusselt no in experimental work and simulated work 81

NOMENCLATURE

General Terms

r	-	Radius
D	-	Diameter
Dh	-	Hydraulic diameter
x	-	Axial/local
A	-	Area
A_c	-	Cross-sectional area
m	-	Mass flow rate
c_v	-	Constant volume specific heat
T	-	Temperature p
q	-	Heat
h	-	Heat transfer coefficient
P	-	Perimeter
L	-	Length/channel length
Nu	-	Nusselt Number
k	-	Thermal conductivity
ΔT_{lm}	-	Log mean temperature difference
Nu	-	Average Nusselt number
α	-	Thermal diffusivity
Re	-	Reynolds number
ρ	-	Density
μ	-	Dynamic viscosity
Pr	-	Prandtl number
ν	-	Kinematic Viscosity
θ	-	Nondimensional temperature
f	-	Friction factor
Kn	-	Knudsen number
Δp	-	Pressure drop
K	-	Loss coefficient
α^*	-	Channel aspect ratio
W	-	Channel width
H	-	Channel depth

CHAPTER 1

Introduction

- Ø ***Major concern areas***
- Ø ***Current Methods Used in Industry***
- Ø ***Microchannel Heat Sink***
- Ø ***Objective of the Work***
- Ø ***Organization of the Thesis***

1.1 Introduction

As the recent research initiatives has been focused to miniaturization in size and increase of efficiency of micro-chips so on a small chip 10^5 to 10^8 components leads to such a high heat generation level of 100W/cm^2 that its temperature removal is major concern for safety and reliability of electronic devices .Heat generation is an irreversible Process and heat must be removed in order to maintain the continuous operation. Microchannel cooling technology was first put forward by Tuckerman and Pease. They circulate water in microchannel fabricated in silicon chips, able to reach the heat flux of 790W/cm^2 without a phase change on penalty in pressure drop of 1.94 bar. The thermal energy developed during the relentless operation of electronics chips is to be dissipated by incorporating efficient heat sinks on the chips. During the yesteryears; it has been observed that the chip failures are caused due to temperature rise in the circuits. This happens because of accumulation of heat. Hence the micro channel embedded chips are the solution in ultra compact electronics gadgets.

Since the development of the first electronic digital computers in the 1940s, the effective removal of heat has played a key role in ensuring the reliable operation of successive generations of computers. The Electrical Numerical Integrator and Computer (ENIAC), dedicated in 1946, has been described as a ‘‘30 ton, boxcar-sized machine requiring an array of industrial cooling fans to remove the 140 KW dissipated from its 18,000 vacuum tubes’’. As with ENIAC, all early computers up to 1957 used vacuum-tube electronics and were cooled with forced air. The invention of the transistor by Bardeen, Brattain, and Shockley at Bell Laboratories in 1947 foreshadowed the development of generations of computers yet to come. As a replacement for vacuum tubes, the miniature transistor generated less heat, was much more reliable, and promised lower production costs. For a while it was thought that the use of transistors would greatly reduce if not totally eliminate cooling concerns. This thought was short-lived as packaging engineers worked to improve computer speed and storage capacity by packaging more and more transistors on printed circuit boards, and then on ceramic substrates.

The trend toward higher packaging densities dramatically gained momentum with the invention of the integrated circuit by Kilby at Texas Instruments and Noyce at Fairchild

Semiconductor in 1959. During the 1960s small scale and then medium scale integration (SSI) and (MSI) led from one device per chip to hundreds of devices per chip. The trend continued through the 1970s with the development of large scale integration (LSI) technologies offering hundreds to thousands of devices per chip, and then through the 1980s with the development of very large scale integration (VLSI) technologies offering thousands to tens of thousands of devices per chip Fig (1.1).

This trend continued with the introduction of the microprocessor. It continues to this day with INTEL and others projecting that a microprocessor chip with a billion or more transistors will be a reality before 2010.

In many instances the trend toward higher circuit density has been accompanied by increased power dissipation per circuit to provide reductions in circuit delay (i.e., increased speed). The need to further increase packaging density and reduce signal delay between communicating circuits led to the development of multi chip modules beginning in the late 1970s and is continuing to this day. Fig.(1.2) represents the chip heat flux and module heat flux. As can be seen the chip heat flux increases at a cumulative growth rate (CGR) of 7 % per year, and heat flux associated with bipolar circuit technologies steadily increased from the very beginning and really took off in the 1980s. There was a brief respite with the transition to CMOS circuit technologies in the 1990s; but the demand for increased packaging density and performance reasserted itself and heat flux is again increasing at a challenging rate.

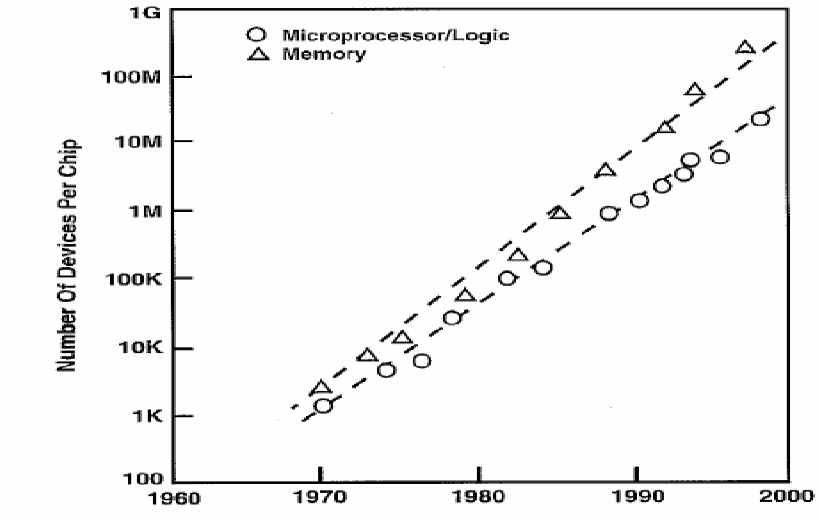

Fig (1.1):- Increase in circuit complexity

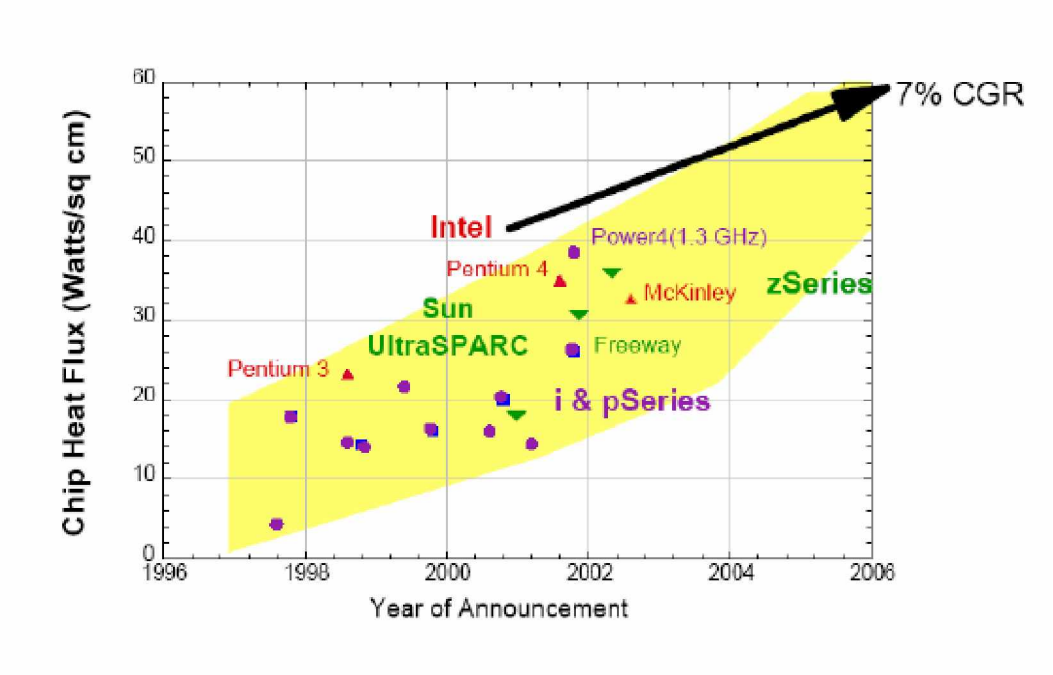

Fig (1.2):- The chronological evolution of chip level Heat Flux

It has been found that for every 2 ºC temperature rise, the reliability of a silicon chip will be decreased by about 10 %. The major cause of an electronic chip failure is due to temperature rise (55%) as against other factors which accounts 20 % vibration, 19 % humidity and 6 % dust Fig.(1.3). So it's a great challenge for the packaging engineers to remove the heat from the electronics chips very effectively.

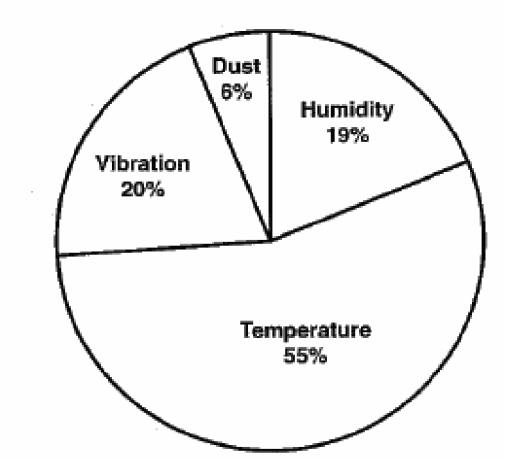

Fig (1.3):- Major Causes of Electronics Failure

Throughout the past 50 years, cooling and thermal management have played a key role in accommodating increases in power while maintaining component temperatures at satisfactory levels to satisfy performance and reliability objectives. Thermal management will play a pivotal role in the coming decade for all types of electronics products. Increased heat fluxes at all levels of packaging from chip to system to facility pose a major cooling challenge. To meet the challenge, significant cooling technology enhancements will be needed in each of the following areas:-

Thermal interfaces, Heat spreading, Air cooling , Indirect and direct water cooling Immersion cooling Refrigeration cooling Thermoelectric cooling Data center cooling
So the thermal design requirements to meet the growing demands are as follows, it is here Traditional Thermal Design Requirements are explained and categorized as follows:-
Design for Performance , Design for Reliability, Design for Serviceability, Design for Extensibility , Design for minimal Cost and Design on minimal Impact on User.

1.2 New Thermal Design Technology

- Design for improved cool ability at the package level via optimized internal thermal conduction paths.
- Design for direct air cooling at the product level via enhanced convection process over the packages.
- Design for special cooling needs at the module level via spot cooling devices attached to the packages.
- Design for low temperature applications- Sub ambient to cryogenic.
- Design for low cost via computer aided thermal engineering (CATE) and improved manufacturability.

1.3 Current Methods Used in Industry

Here are the various types of methods used in electronics (Computer) industry to cool Modules, Systems, and Data centers

1.3.1 Module Level Cooling

Processor module cooling is typically characterized in two ways: cooling internal and external to the module package and applies to both single and multi chip modules. Fig (1.4)

illustrates the distinction between the two cooling regimes in the context of a single-chip module.

1.3.1.1 Internal Module Cooling

The primary mode of heat transfer internal to the module is by conduction. The internal thermal resistance is therefore dictated by the module's physical construction and material properties. The objective is to effectively transfer the heat from the electronics circuits to an outer surface of the module where the heat will be removed by external means which will be discussed in the following section.

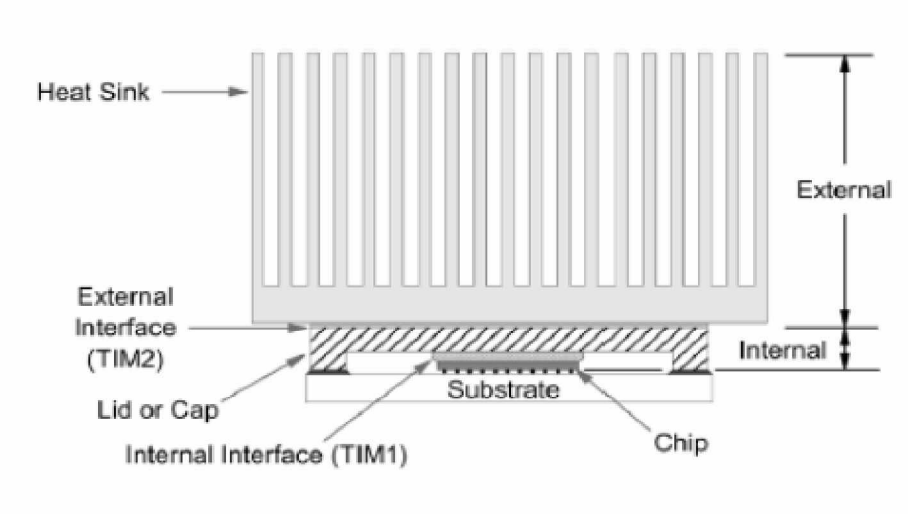

Fig (1.4):- Cross Section of a typical Module Denoting Internal Cooling Region and External Cooling Region

1.3.1.2 External Module Cooling

Cooling external to the module serves as the primary means to effectively transfer the heat generated within the module to the system environment. This is accomplished primarily by attaching a heat sink to the module by Wu.and Little . Traditionally, and preferably, the system environment of choice has been air because of its ease of implementation, low cost, and transparency to the end user or customer. This section, therefore, will focus on air-cooled heat sinks. Liquid-cooled heat sinks typically referred to as cold plates will also be discussed.

1.3.1.3 Immersion Cooling

Immersion cooling has been of interest as a possible method to cool high heat flux components for many years. Unlike the water-cooled cold plate approaches which utilize physical walls to separate the coolant from the chips, immersion cooling brings the coolant in direct physical contact with the chips. As a result, most of the contributors to internal thermal resistance are eliminated, except for the thermal conduction resistance from the device junctions to the surface of the chip in contact with the liquid. Direct liquid immersion cooling offers a high heat transfer coefficient which reduces the temperature rise of the heated chip surface above the liquid coolant temperature. The magnitude of the heat transfer coefficient depends upon the thermo-physical properties of the coolant and the mode of convective heat transfer employed. The modes of heat transfer associated with liquid immersion cooling are generally classified as natural convection, forced convection, and boiling. Forced convection includes liquid jet impingement in the single phase regime and boiling (including pool boiling, flow boiling, and spray cooling) in the two-phase regime.

1.3.2 System-Level Cooling

Cooling systems for computers may be categorized as air-cooled, hybrid-cooled, liquid-cooled, or refrigeration- cooled. An air-cooled system is one in which air, usually in the forced convection mode, is used to directly cool and carry heat away from arrays of electronic modules and packages. In some systems air-cooling alone may not be adequate due to heating of the cooling air as it passes through the machine. In such cases a hybrid-cooling design may be employed, with air used to cool the electronic packages and water-cooled heat exchangers used to cool the air. For even higher power packages it may be necessary to employ indirect liquid cooling. This is usually done utilizing water-cooled cold plates on which heat dissipating components are mounted, or which may be mounted to modules containing integrated circuit chips. Ultimately, direct liquid immersion cooling may be employed to accommodate high heat fluxes and a high system heat load.

1.3.2.1 Air Cooling

Although liquid forced convection and boiling offer the highest heat transfer rates, air cooling has been and continues to be the most widely used technique for heat rejection. The principal advantages of cooling with air are its ready availability and ease of application. Prior to 1964, all computers were cooled solely by forced air. Air moving devices took in room air and provided a serial flow of air over columns of boards carrying printed circuit cards with single chip modules. In many cases air moving devices at either the bottom or top of a column of boards provided sufficient cooling air flow. A push–pull airflow arrangement with air moving devices at both the bottom and top of the column of boards was used for those cases requiring higher pressure drop capability.

Forced air-cooled systems may be further subdivided into serial and parallel flow systems. In a serial flow system the same air stream passes over successive rows of modules or boards, so that each row is cooled by air that has been preheated by the previous row. Depending on the power dissipated and the air flow rate, serial air flow can result in a substantial air temperature rise across the machine. The rise in cooling air temperature is directly reflected in increased circuit operating temperatures. This effect may be reduced by increasing the air flow rate. Of course to do this requires larger blowers to provide the higher flow rate and overcome the increase in air flow pressure drop. Parallel air flow systems have been used to reduce the temperature rise in the cooling air. In systems of this type, the printed circuit boards or modules are all supplied air in parallel. Since each board or module is delivered its own fresh supply of cooling air, systems of this type typically require a higher total volumetric flow rate of air.

1.3.2.2 Hybrid Air-Water Cooling

An air-to-liquid hybrid cooling system offers a method to manage cooling air temperature in a system without resorting to a parallel configuration and higher air flow rates. In a system of this type, a water-cooled heat exchanger is placed in the heated air stream to extract heat and reduce the air temperature. The cooling system incorporated an air-to-water finned tube heat exchanger between each successive row of circuit boards. The modules on the boards were still cooled by forced convection with air, however; the heated

air exiting a board passed through an air-to-water heat exchanger before passing over the next board. Approximately 50% of the heat transferred to air in the board columns was transferred to the cooling water. Ultimately air-to-liquid hybrid cooling offers the potential for a sealed, recirculation, and closed-cycle air-cooling system with total heat rejection of the heat load absorbed by the air to chilled water. Sealing the system offers additional advantages. It allows the use of more powerful blowers to deliver higher air flow rates with little or no impact on acoustics. In addition, the potential for electromagnetic emissions from air inlet/outlet openings in the computer frame is eliminated. Another variant of the hybrid cooling system is the liquid-to-air cooling system. In this system liquid is circulated in a sealed loop through a cold plate attached to an electronic module dissipating heat. The heat is then transported via the liquid stream to an air-cooled heat exchanger where it is rejected to ambient air. This scheme provides the performance advantages of indirect liquid cooling at the module level while retaining the advantages of air cooling at the system or box level. Most recently, a liquid-to-air cooling system is being used to cool the two processor modules in the Apple Power Mac G5 personal computer shipped earlier this year.

1.3.2.3 Liquid-Cooling Systems

Either the air-to-water heat exchangers in a hybrid air–water-cooled system or the water-cooled cold plates in a conduction-cooled system rely upon a controlled source of water in terms of pressure, flow rate, temperature, and chemistry. In order to insure the physical integrity, performance, and long-term reliability of the cooling system, customer water is usually not run directly through the water-carrying components in electronic frames. This is because of the great variability that can exist in the quality of water available at computer installations throughout the world. Instead a pumping and heat exchange unit, sometimes called a coolant distribution unit (CDU) is used to control and distribute system cooling water to computer electronics frames. The primary closed loop (i.e., system) is used to circulate cooling water to and from the electronics frames. The system heat load is transferred to the secondary loop (i.e., customer water) via a water-to-water heat exchanger in the CDU. Within an electronics frame a combination of parallel-series flow networks is used to distribute water flow to individual cold plates and heat exchangers. Water flow in the primary loop is provided at a fixed flow rate by a single operating pump, with a stand-by pump to provide uninterrupted operation if the operating pump fails. The temperature of the

water in the primary loop is controlled by using a mixing valve to regulate the fraction of the flow allowed to pass through the water-to-water heat exchanger and forcing the remainder to bypass the heat exchanger. A CDU is also required for direct immersion cooling systems. In addition, because of the relatively high vapor pressure of the coolants suitable for direct immersion applications (e.g., fluorocarbons), the cooling system must be both "vapor-tight" and "liquid-tight" to ensure against any loss of the relatively expensive coolant.

1.3.2.4 Refrigeration Cooled Systems

The potential for enhancement of computer performance by operating at lower temperatures was recognized as long ago as the late 1960s and mid-1970s. Some of the earliest studies focused on Josephson devices operating at liquid helium temperatures (4K). The focus then shifted to CMOS devices operating near liquid nitrogen temperatures (77 K). A number of researchers have identified the electrical advantages of operating electronics all the way down to liquid nitrogen temperatures (77 K). In summary, the advantages are:

- Increased average carrier drift velocities (even at high fields);
- Steeper sub-threshold slope, plus reduced sub-threshold currents (channel leakages) which provide higher noise margins;
- Higher transconductance;
- Well-defined threshold voltage behavior;
- No degradation of geometry effects;
- Enhanced electrical line conductivity;
- Allowable current density limits increase dramatically (i.e., electro migration concerns diminish).

1.3.3 Data Center Thermal Management

Due to technology compaction, the information technology (IT) industry has seen a large decrease in the floor space required to achieve a constant quantity of computing and storage capability. However, the energy efficiency of the equipment has not dropped at the same rate. This has resulted in a significant increase in power density and heat dissipation

within the footprint of computer and telecommunications hardware. The heat dissipated in these systems is exhausted to the room and the room has to be maintained at acceptable temperatures for reliable operation of the equipment. Cooling computer and telecommunications equipment rooms is becoming a major challenge. The increasing heat load of data-com equipment has been documented by a thermal management consortium of 17 companies and published in collaboration with the Uptime Institute as shown in Fig. (1.5).

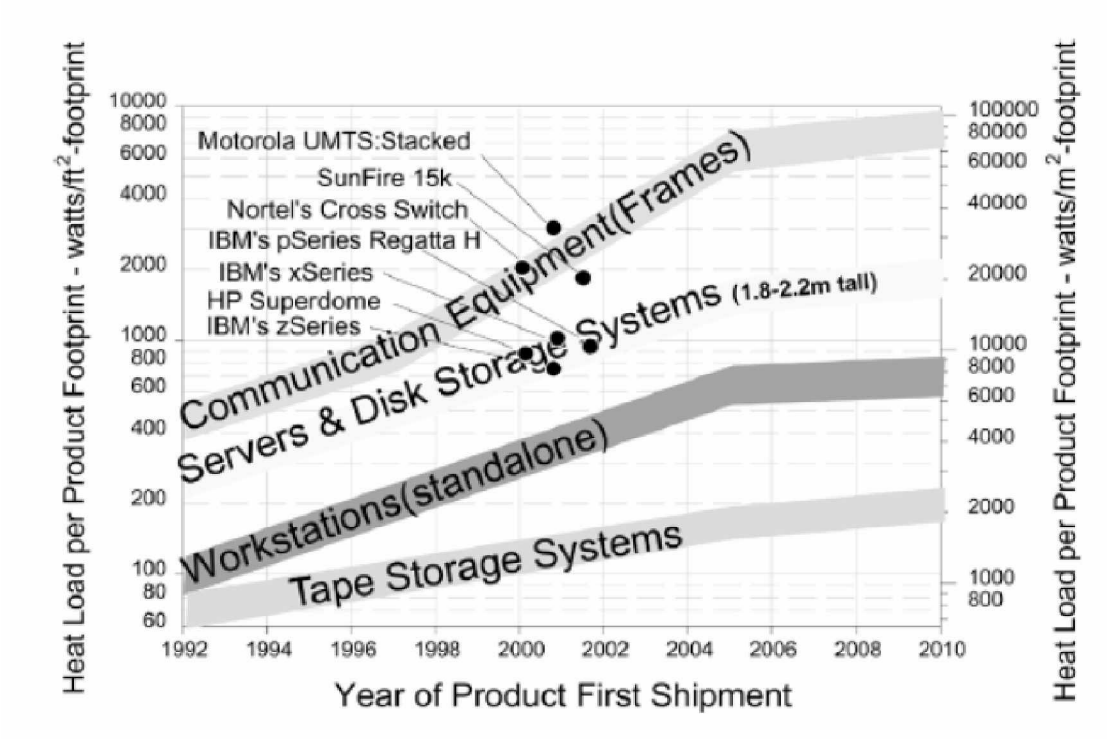

Fig (1.5):- Heat Load per product Foot Print

Also shown here the measured heat fluxes (based on product footprint) of some recent product announcements. The most recent shows a rack dissipating 28500 W resulting in a heat flux based on the footprint of the rack of 20900 W/m. With these heat loads the focus for customers of such equipment is in providing adequate air flow at a temperature that meets the manufacturer's requirements.

Heat removal has become an important factor in the advancement of microelectronics due to drastically integrated density of chips in digital devices and increased current-voltage handling capability of power electronic devices by Peng. Micro-channel heat sinks remove heat 50 times more efficiently than conventional methods. However, one-layered micro-

channel heat sinks induce high temperatures which can produce thermal stress on the chips and packages. To avoid such high temperatures, a large pressure drop is necessary which moves the coolant through the cooling channels more rapidly, thus requiring a larger, noisier pumping system. Scientists at The Ohio State University have developed a multi-layered microchannel heat sink with a current flow arrangement for cooling that is a substantial improvement over conventional one-layered micro-channel heat sink designs. The thermal performance and the temperature distribution for these types of micro-channels were analyzed and a procedure for optimizing the geometrical design parameters was developed. While the power supply system of the multi-layered design is not significantly more complicated than the one-layered design, the stream-wise temperature rise on the base of surface was substantially reduced.

At the same time, the pressure drop required for the multi-layered heat sink was substantially smaller than the one-layer design. It is shown that the thermal resistance is as low as 0.03 K/W for microchannel heat sinks, which is substantially lower than conventional channel-sized heat sinks.

1.4 Heat Sink

A heat sink is an environment or object that absorbs heat and dissipates heat from another using thermal contact (either direct or radiant).

Application:-

1. Cooling electronics devices like microprocessors, DSPs, GSPs
2. Refrigeration
3. Heat engines

In common use it is metal object brought in to contact with an electronic component's hot surface- though in most cases, a thin thermal interface material mediates between the two surfaces. Microprocessors and power handling semiconductors are examples of electronics that need a heat sink to reduce there temperature through increased thermal mass and heat dissipations (primarily by conduction and convection and to a lesser extend by radiation.

1.5 Micro channel Heat Sink

Micro channel heat sinks feature a high convective heat transfer coefficient, which is particularly beneficial to high end electronics cooling.

1.5.1 Design Parameters

The design parameters include the heat sink material, the number and geometry of the fins and their alignment and the base plate thickness as shown in Fig. (1.6). In order to obtain the minimum thermal resistance and pressure drop, each of these parameters must be designed well.

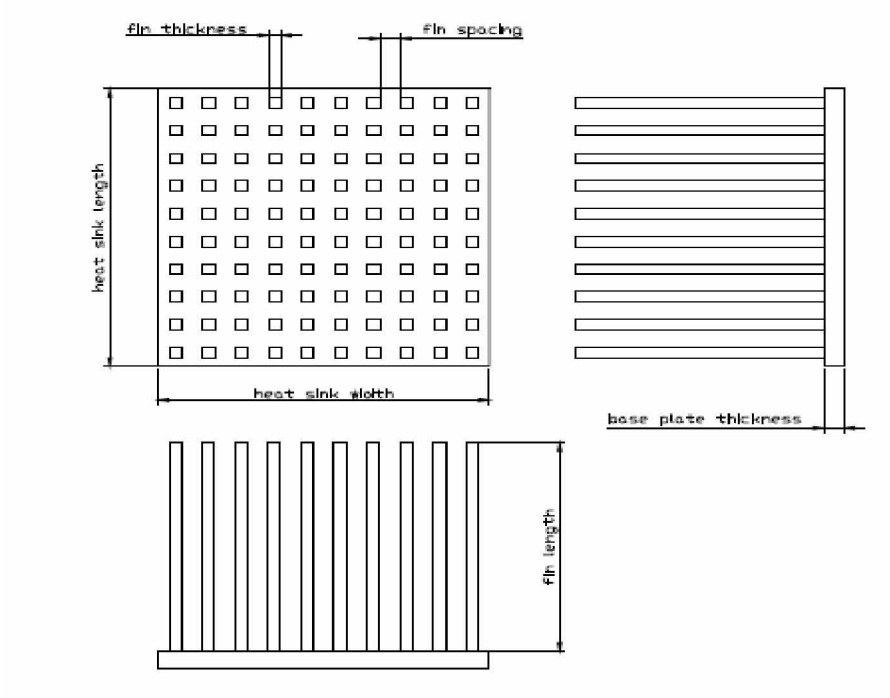

Fig (1.6):- Heat Sink Design Parameters

1.5.2 Heat Sink Material

Heat sinks are made from a good thermal conductor such as copper or aluminum alloy. Copper (401 W/m K at 300 K) is significantly more expensive than aluminum (237 W/m K at 300 K) but is roughly twice as efficient as thermal conductor. Aluminum has the significant advantage that it can be easily formed by extraction, thus making complex cross-sections possible. Aluminum is also much lighter than copper, offering less mechanical stress

on delicate electronic components. Some heat sinks made from aluminum have a copper core as a trade off as in Swiftech 462-A heat sink . Although the thermal conductivity of zinc is lower compared to that of aluminum and copper, it may also be a good material for electronic cooling purposes Figure (1.7). When zinc added to an alloy, it eliminates porosity in the casting process, which is an advantage over aluminum and copper since they are not pore free after the casting.

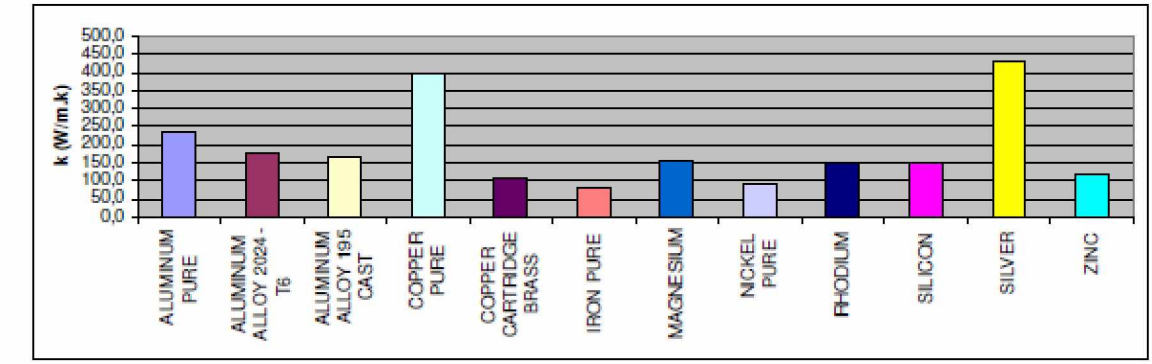

Fig (1.7):- Thermal conductivities of common heat sink materials and possible candidates

1.5.3 The number of the fins

A heat sink usually consists of a base with one or more flat surfaces and an array of comb or fin-like protrusions to increase the heat sink's surface area contacting the air, and thus increasing the heat dissipation rate. In Fig (1.8) Cu MHE with channels molded, plenums cut, and holes drilled is measured in micro level.

It is one of the most important factors for heat sink performance. A heat sink designed for electronics cooling is a compact heat exchanger for which the ratio of heat transfer area to occupied volume is very large. Therefore increasing the number of fins provides more area for heat transfer. Increasing the number of fins from 238 to 294, Hedgehog increased the heat transfer area by 8.4 % and approximately 10 % efficiency is assured in the succession of Hedgehog-238M to Hedgehog-294M. However, it should be noted that increasing the number of fins creates an adverse effect, which is the increased static pressure drop. In order to overcome higher pressure drops, higher pumping powers are needed, which requires the installation of more powerful fans or blowers.

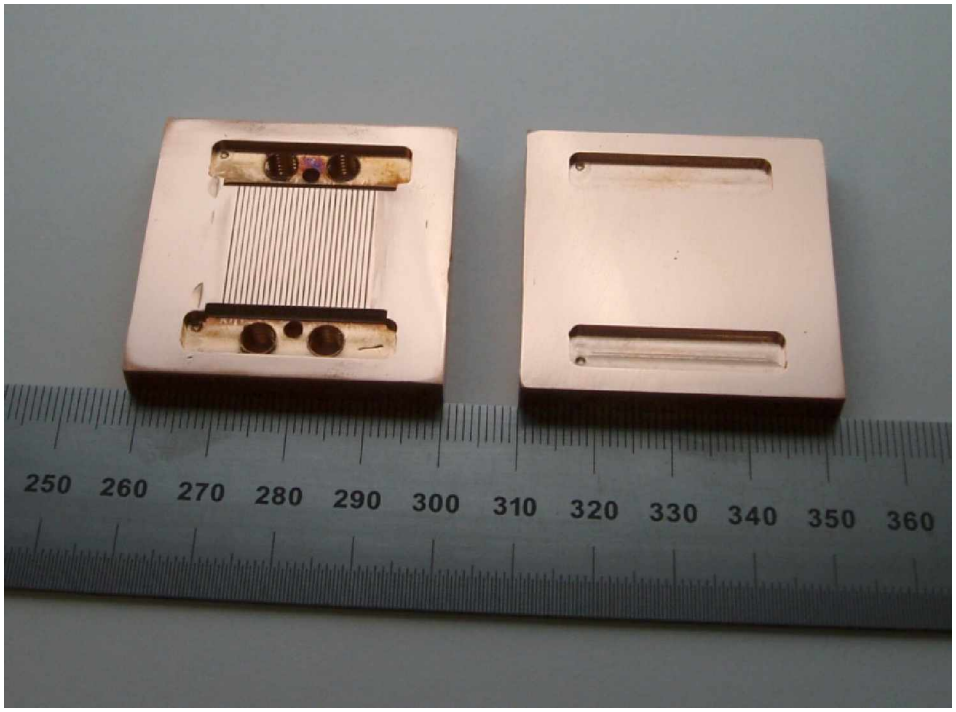

Fig (1.8): Cu MHE with channels molded, plenums cut, and holes drilled

1.5.4 Fin Shapes

Different kinds of heat sink geometries are possible. Pin fins, straight fins, fluted fins, wavy fins and fins with non-standard geometry are possible. The most common ones are pin fins whose cross section can be round, square, elliptical, hexagonal or any other suitable geometry. A round cross section pin fin heat sink design is used in Global Win CDK38 Fig (1.9). Straight fins that have rectangular cross sections are also widely used. Depending on the spacing among the fins of a heat sink, flow requirements and pressure drops may differ.

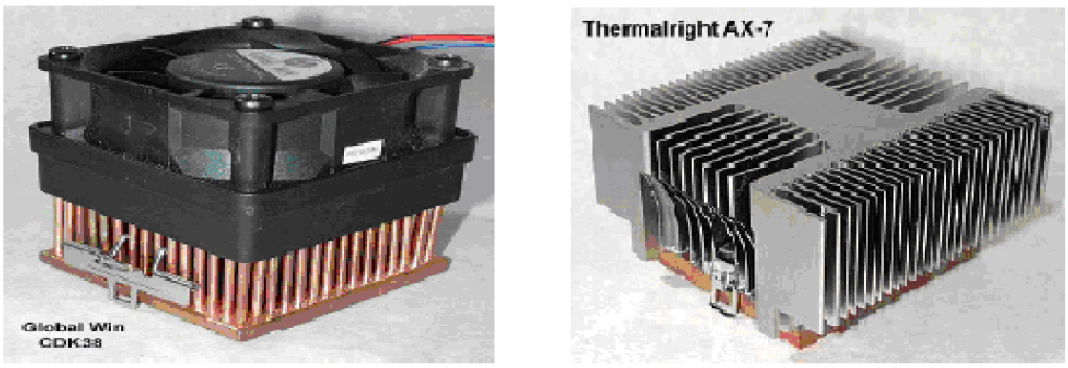

Fig (1.9):- Two Heat Sinks with different fin geometry

1.5.5 Other Parameters

A fan often aids a heat sink by providing increased airflow over the heat sink — thus maintaining a larger temperature gradient by replacing the warmed air more quickly than passive convection achieves alone — this is known as a forced air system. If a fan is specified for a system, pressure drop, volumetric flow rate and flow cross sectional area also become system constraints. Otherwise they are the design parameters.

Pressure drop :- Pressure drop is the resistance to the air movement and it is related with flow cross sectional area, fin spacing and fin length. The heat sink should be designed so as to yield a smaller pressure drop than the static pressure of the fan. The heat sink selected or designed changes the total pressure drop of the system, although it is not a very major difference, the operating point which is the intersection of the system impedance curve and the fan impedance curve may shift.

Volumetric flow rate **:-** Volumetric flow rate is the velocity times the cross sectional area of the flow. Velocity magnitude of the incoming air is the dominant factor creating turbulence. Therefore if the fan is specified, the velocity of the air and the flow regime are known. Flow inlet velocity as a design parameter is also surveyed in the literature. Increasing the flow inlet velocity thus the volumetric flow rate, which results in turbulence, the thermal resistance may be reduced by 35 % compared to the same geometry with laminar flow.

Flow cross sectional area :- Flow cross sectional area is known as long as the fan dimensions are known. Designing a heat sink with a smaller cross sectional area than the flow area creates the by-pass of air. Since some of the air delivered by the fan will not participate in the heat transfer, efficiency is reduced. Ducting the coolant fluid to and from the heat sink through tubes, it is demonstrated that larger heat removal capabilities are achievable as the by-pass of air is prevented.

1.6 Objective of the Work

In present study a numerical model with fully developed flow is presented and used to analyze three dimensional microchannel heat sink for Re numbers (< 160 with hydraulic diameter 86 μm). In the current investigation, three different cases ($qw=90W/cm^2$, $\Delta p=$ 50kpa, 15kpa, and 10kpa) were considered .we examine it for heat flux for 50 W/cm^2,90 W/cm2 and 150W/cm^2 . The average Nusselt number is carefully defined and after a series of calculations for different total pressure drops in the channel the relation between the Nusselt number and the Reynolds number is analyzed and plotted The numerical model is based on three dimensional conjugate heat transfer

FLUENT, a commercial package employs continuum model of Navier Stokes with SIMPLE algorithm, is used for this investigation. The numerical solver codes are well-established and thus provide a good start to more complex heat transfer and fluid flow problems. FLUENT provides adaptability to variation of thermo physical properties with respect to temperature effect. The thermo physical properties are chosen at a reference temperature A series of calculations were carried out to analyze rectangular silicon-based microchannel heat sink with a geometry Computations were performed for different total pressure drops in the channel to obtain the relation between the overall averaged Nu number and the Re number for this specific geometry of heat sinks

1.7 Organization of the Thesis

This thesis has been organized in total five chapters. Chapter 1 and 2 is for foundation of the subject; chapter-3 is for mathematical formulation, while chapter-4 is for results, discussions and conclusion; last chapter is references.

CHAPTER 2

Literature Review

- *Introduction*
- *Microchannel Concepts*
- *Analytical studies*
- *Numerical studies*
- *Experimental studies*
- *Closure*

2.1 Introduction

Compact heat exchanger constitutes geometrically complex heat flow paths that pose enormous difficulty to the attempt to perform thermal analysis. In the industry today, Computational Fluid Dynamics (CFD) codes are widely used as a tool of thermal analysis. CFD solutions of high spatial and temporal resolutions can be obtained on a desktop computer or even a laptop. However, CFD-based thermal analysis is not necessarily easy to perform where the object of analysis is geometrically complex. Before embarking on CFD analysis the analyst has to devise a model, omitting some geometric features of structures and approximating complex configurations by simpler ones. This first phase of analysis is an art that often determines the accuracy of the end result no matter how rigorously the subsequent CFD analysis is performed. Although CFD code vendors are providing the tools for the user to set up pre-CFD models and generate meshes, the modeling still remains in the realm of art, increasingly difficult art with the growth of geometric complexity in the system box. Even after some simplifications, the model tends to be complex, reflecting the situation in the actual equipment. The CFD simulation on such a model involves a large number of meshes and, thus, requires a powerful computer and long computing time. Also, the analyst often has to iteratively search for a better mesh system to improve the confidence in the simulation result, and such a search is time consuming where heat transfer paths are complex. So, with the progress of compact packaging, the time and the computational resource required for CFD-based thermal analysis are increasing.

With the advent of Computational Fluid Dynamics (CFD) in the recent years, flow and heat transfer computations have become quite readily possible. In particular, with the recent introduction of high power workstations and personal computers the cost of such computations has been drastically reduced and as a result many CFD codes have come into the market. More recently, such computations have become very popular in the application area of cooling of electronic components. In fact, this popularity has led to several purposes developed CFD codes coming into the market which are specifically tailored for use by heat transfer engineers in the electronic industry. The relatively recent adoption of CFD simulation studies in electronic cooling applications has prompted some interest in validation of these codes for these types of problems. In general, validation and benchmarking of CFD

codes has been an on-going research area attracting a lot of attention from both users and code developers.

Studies on micro channel flows in the past decade are categorized in to various topics. The literature survey extends over a wide range of topics such as measurement and estimation of friction factor and heat transfer in micro channels and small-diameter tubes, comparison with flow in conventional channels, investigation single-phase boiling and two-phase flow in microchannels, minichannels and small tubes, gas flow in micro channels, analytical studies on micro channel flows and design and testing of micro channel heat sinks for electronics cooling. For each study, key descriptors of the cooling configuration and the primary observations are included.

2.2 Micro channel Concepts

Standard semiconductor fabrication techniques were applied to construct the first silicon micro channels in the 1980's. In 1981, Tuckerman and Pease(1) used silicon micro channels, with water as the working fluid, to dissipate power from an electronic chip. The micro channels were etched in a silicon sample with an overall dimension of $1cm^2$. They had a channel width of approximately 60 μm and a parameterized channel height varying between 287 μm and 376 μm. These micro channels effectively dissipated up to 790 W/cm^2 while maintaining a chip temperature below 110 °C . The small characteristic length scale of silicon micro channels prompted the scientific community to investigate the possibility of new transport physics.

Shortly after Wu and Little (2) obtained experimental results for fluid flow in microchannels for gas flow. Their measured friction factors in the laminar regime were higher than expected, and they found that the transition Reynolds number ranged from 350 to 900. Peng (3) conducted experiments on microchannels, and they found that the laminar-to-turbulent transition period occurred at Reynolds numbers which were lower than expected from conventional theory. Peng and Peterson found disparities between conventional flow theory and experimental results for microchannels. They tested microchannels with hydraulic diameters ranging from133 μm to 367 μm, and they showed a friction factor dependence on hydraulic diameter and channel aspect ratio (4)

Judy (5) did pressure drop experiments on both round and square microchannels with hydraulic diameters ranging from 15 to 150 μm. They tested distilled water, methanol and isopropanol over a Reynolds number range of 8 to 2300. Their results showed no distinguishable deviation from laminar flow theory for each case. Liu and Garimella (6) conducted flow visualization and pressure drop studies on microchannels with hydraulic diameters ranging from 244 to 974 μm over a Reynolds number range of 230 to 6500. They compared their pressure drop measurements with numerical calculations. Computations were performed for different total pressure drops in the channel to obtain the relation between the overall averaged Nu number and the Re number for this specific geometry of heat sinks. Choi (7) also suggested by their experiments with microchannels inside diameters ranging from3 to 81μm that the Nusselt number did in fact depend on the Reynolds number in laminar microchannel flow. Experimental measurements for pressure drop and heat transfer coefficient were done by Rahman (8) he use water as a working fluid and tests are conduct on channel of different depths.

With the advancements of computing in the past few decades, electronics have become faster, smaller, and more powerful, resulting in an ever-increasing strain on the device's cooling system. Dr. Gordon Moore stated that, "semi-conductor transistor intensity, and hence performance, doubles roughly every 18 months ", meaning that the amount of heat requiring dissipation proportionately increases. This observation can be seen in the majority of today's personal computers (PC) chips. In most cases, the chips are cooled through the use of forced air convection fans . However, when dealing with components that contain billions of transistors, working at high frequencies (a few GHz), temperatures can reach critical levels where standard-cooling methods are not sufficient. In an effort to improve methods for high heat flux cooling, liquids were forced through micro-channels manufactured within the component.

To understand water convection, one must have comprehensive knowledge of theoretical concepts of energy and heat transfer. Heat transfer is energy in transit due to a change in temperature. There are several different modes for heat transfer: conduction, convection, boiling, condensation and radiation . In the carried out experiment, convection was the primary mode. Convection is heat transfer between a surface and a fluid in motion,

such as water or air, when the fluid and the surface have a temperature difference. When dealing with convective heat transfer q'' represents heat flux (W/cm^2).

In single-phase flow water remains in the liquid state. In order to calculate the convective heat flux in a single-phase flow, one must monitor the mass flow rate and measure the difference of outlet and inlet temperatures of water contained in the cooling system, $q'' = mC_p(T_{out} - T_{in})$.The aforementioned equation will provide the basic tools for interpreting and better understanding the significance of the acquired data.

Microchannel heat sink was first proposed for heat sinking of very large scale integrated (VLSI) electronic components in 1980s. Tukerman and pease reported a microchannel heat sink, consisting of parallel micro flow passages 50 μm wide and 302 μm deep, which was demonstrated to have thermal resistance as low as 9×10^{-6} $K/(W/m^2)$ for a pumping power 1.84 W. At a heat flux of 790 W/cm^2, this corresponds to a maximum temperature difference of 71^o C. This work was considered as a milestone in the development of micro-scale heat sinks; however, typical pressure drop for these microchannels is more than two bars. Mean while the surface temperature rises due to caloric heating along the flow direction is also very large which is highly undesirable from the performance and reliability point of view.

Non-uniform Temperature Distribution in Electronic Devices Cooled by Flow in Parallel Micro-Channels, was discussed by Judy and Maynes (9).Two-Phase Flow Patterns in Parallel Micro-Channels, was studied by Lie and Garimella (10).

Mainfold microchannel heat sinks were first suggested by choi and Barron(11) and numerically studied by Rahman and Fedorov (12). Compared to conventional microchannel heat sinks, manifold microchannel heat sinks feature many inlet and outlet manifolds, alternating at a periodic distance along the length of the microchannels. Coolant flows from the inlet port in to the manifolds and forms separate streams. Each stream flow through a short section of microchannels. If fully developed laminar flow fixed flow rate are assumed, at the pressure drop is reduced by a factor equal to the number of manifold inlet/outlet compared with conventional microchannel heat-sink, on the other hand the same temperature

variation exists for manifold microchannel in a much shorter distance. There are also concerns on the heat transfer efficiency for the region underneath the manifolds.

Assuming fully developed conditions, Le (13) conducted an optimization study to minimize the temperature gradient and the maximum temperature for microchannel heat sink. It was demonstrated that further reduction in maximum temperature and temperature gradient could be achieved by verying the cross-sectional dimensions of the microchannel. The penalty of this method is the dramatically increased pressure drop due to the acceleration along the flow direction.

J. Li and G.P. Peterson (14) numerically simulated a forced convection heat transfer occurring in silicon based micro channel heat sinks has been conducted using a simplified three-dimensional conjugate heat transfer model (2D fluid flow and 3D heat transfer) consists of a 10 mm long silicon substrate, with rectangular micro channel, 57 μm wide and 180 μm deep, fabricated along entire length with hydraulic diameter 86 μm. The influence of the geometric parameters of the channel and thermo physical properties of the fluid on the flow and the heat transfer, are investigated using temperature dependent thermo physical property method. Result indicates that this properties of the liquid can significantly influence both the flow heat transfer in the micro channel heat sink. The result indicates that the variations in the way the Nusselt number is defined may results in different conclusions even using the same experimental data. Then compare the numerical results with other published numerical results and experimental data available in literature.

In the past twenty-three years strenuous research has been repeatedly conducted to better understand single and two-phase flow mechanisms of micro-channel chips. In an attempt to counter current flow arrangement for the cooling of electronic components Vafai (15) compared the thermal performance of two layer micro-channel heat sinks with single layer conventional heat sinks. It was found that counter-flow arrangement reduces the temperature gradient dramatically compared with single-layered micro channel for Re = 144. Micro channel heat sinks were discussed in Wei and Joshi (16). By stacking several layers of micro channels, the total available flow area increases. For fixed flow rate, the pressure drop is reduced by a factor almost equal to the number of layers. The thermal performance of the stacked micro channel heat sink is affected by the channel aspect ratio, the thermal

conductivity of the base material and the flow rate. A simple thermal-resistance-network analysis found that affixed pumping power the overall the thermal resistance for a two layer micro channel is 30% less than that of single layered micro channel dimensions on different layers and to adjust the flow directions and interlayer flow rate ratio for different power map of microprocessors.

2.3 Analytical studies

Gui and Anderson (17) presented an analytical approach for characterizing electronic packages, based on the steady-state solution of the Laplace equation for general rectangular geometries, where boundary conditions are uniformly specified over specific regions of the package.. The basis of the solution is a general three dimensional Fourier series solution which satisfies the conduction equation within each layer of the package. The application of boundary conditions at the fluid-solid, package board and layer-layer interfaces provides a means for obtaining a unique analytical solution for complex IC packages. They compared the values with published experimental data for both a plastic quad flat package and a multichip module to demonstrate that an analytical approach can offer an accurate and efficient solution procedure for the thermal characterization of electronic packages.

Davies (18) presented the method to correct the thermal resistance of electronics components is to adjust the junction-to-ambient thermal resistance to account for operational conditions. For forced convection applications, they proposed two factors; the first accounts for any upstream aerodynamic disturbance and the second addresses purely thermal interaction. Thus if an upstream powered component interacts with a downstream component, the two factors are combined. They found that both factors may be quantified in terms of readily measured temperatures and then used as coefficients to adjust the standard thermal resistance data for operational conditions. They applied this approach to a symmetrical array of board mounted 160-lead devices and the data shows how the factors vary with component position, non-dimensional power distribution and Reynolds number. Based on data they proposed a new method of generating operational component thermal resistances.

Pucha (19) presented a field-use induced damage mapping methodology that can take into consideration the field-use thermal environment profile to develop accelerated thermal cycling guidelines for packages intended to be used in military avionics thermal environment. They considered the board-level assembly process mechanics and critical geometric features with appropriate material models while developing the methodology. The models they developed are validated against in-house and published accelerated thermal cycling experimental data. The developed mapping methodology was employed to design alternate accelerated thermal cycles by matching the creep and plastic strain contributions to total inelastic strain accumulation in solder under military field-use and accelerated thermal cycling environments, while reducing the time for accelerated thermal cycling and qualification.

Zhao (20) presented an analytical and numerical study on the heat transfer characteristics of forced convection across a micro channel heat sink. Two analytical approaches are used by them: the porous medium model and the fin approach. In the porous medium approach, the modified Darcy equation for the fluid and the two-equation model for heat transfer between the solid and fluid phases are employed. Firstly, the effects of channel aspect ratio (as) and effective thermal conductivity ratio on the overall Nusselt number of the heat sink are studied in detail. The predictions from the two approaches both show that the overall Nusselt number (Nu) increases as *s*α increased and decreases with increasing k.. The effect of porosity (e) on the thermal performance of the micro channel was also examined by them. They found that, whereas the porous medium model predicts the existence of an optimal porosity for the micro channel heat sink, the fin approach predicts that the heat transfer capability of the heat sink increases monotonically with the porosity. They also studied the effect of turbulent heat transfer within the micro channel, and they found that turbulent heat transfer results in a decreased optimal porosity in comparison with that for the laminar flow. They proposed a new concept of micro channel cooling in combination with micro heat pipes, and the enhancement in heat transfer due to the heat pipes is estimated. Finally, they conducted two-dimensional numerical calculations for both constant heat flux and constant wall temperature conditions to check the accuracy of analytical solutions and to examine the effect of different boundary conditions on the overall heat transfer.

Chen (21) developed an effective method for predicting and optimizing the thermal performance of heat sinks with Parallel-Plain Fin under a given design constraint of pressure drop. They developed the thermal and hydrodynamic performance analyzers for PPF heat sinks. A screening experimental design using the Taguchi method has been performed to determine key factors that are critical to the design and screen out unimportant design factors; and a Response

Surface Methodology is then applied to establish analytical models for the thermal resistance and pressure drop in terms of the key design factors with a CCD experimental design. By employing the Sequential Quadratic Programming technique, a series of constrained optimal designs can be efficiently performed. After comparing between these predicted optimal designs and those evaluated by the theoretical calculations the agreement they got was satisfactory.

Modeling of transport in micro channels can be divided in to two categories. In the first, method used for macro-scale channels are directly implemented to evaluate the performance of micro channel heat sinks. In the second category, new effects are taken into account to explain the deviation of the measured results from classical theory. The former range from simple 1-D models to three dimensional conjugate studies (Weisberg and Bau (22) ,Yin and Bau (23), Fedorov and Visakanta (24). However, existing analytical studies are still inconclusive.

Analysis of micro channel heat sinks for electronics cooling was discussed by C.Y. Zhao (25) this paper presents an analytical and numerical study on the heat transfer characteristics of forced convection across a microchannel heat sink. Two analytical approaches are used: the porous medium model and the fin approach. Firstly, the effects of channel aspect ratio (a_s) and effective thermal conductivity ratio (k) on the overall Nusselt number (Nu) increases as a_s is increased and decreases with increasing k. However, the results also reveal that there exists significant difference between the two approaches for both the temperature distributions and overall Nusselt numbers, and the discrepancy becomes larger a_s either as or k is increased. It is found that where as the porous medium model predicts the existence of an optimal porosity for the microchannel heat sink, the fin approach predicts that the heat transfer capability of the heat sink increases monotonically with the

porosity. The effect of turbulent within the microchannel is next studied, and it is found that turbulent heat transfer results in a decreased optimal porosity in comparison with that for laminar flow. Finally, two-dimensional numerical calculations are conducted for both constant heat flux and wall temperature conditions to check the accuracy of analytical solutions and to examine the effect of different boundary conditions on the overall heat transfer.

2.4 Numerical studies

Fund and Rector (26), performed numerical simulations to investigate convective-conductive heat transfer due to a laminar boundary layer flow of air over a two dimensional array of rectangular chip blocks which represent the finite heat sources. A time-accurate numerical scheme algorithm, PISO (pressure-implicit with splitting of operators), has been used to simulate the conjugate heat transfer between the fluid and solid phases. The results of the simulations show that the existence of the array of blocks results in stagnant flow regions between blocks in which heat convected to the ambient flow field is limited. It was found that heat transfer can be enhanced passively, especially in the areas between blocks, by opening the chip board between blocks. The enhancement of heat transfer thus occurring is presumably due to a pseudo-suction force which induces a vertical flow between blocks. The enhancement of heat transfer for the chips on-board is reflected by a global increase of the Nusselt number on the chip blocks, especially on the west sides of the chips located further downstream of the flow direction. Further investigation shows that the chip-to-chip temperature variations diminish if the openings located upstream of the front end block and downstream of the rear end block are sealed. The optimal cooling configuration for the array of chip blocks can be utilized by the electronics industry.

Masud (27) tried to validate the CFD package FLUENT with the experimental data obtained by then earlier. Here they have taken a heated chip with temperature 353 K and the air inlet velocity at temperature 293 K. The inlet velocities were varied from 1 m/s to 7 m/s. Various turbulence models have been tested, and the effect of the channel inlet flow on the heat transfer rate has been determined by considering both a uniform and fully-developed condition. The substrate adiabatic heat transfer rate has been determined by considering both

uniform and fully-developed condition. The substrate adiabatic heat transfer coefficient is also numerically determined. The results indicate that the flow in the vicinity of the module is three dimensional, and exhibits flow separation and vortex formation, hence leading to a complex distribution of the local heat transfer coefficient on the substrate. In general the flow structure was in good agreement with the experiments. The predicted turbulence intensity did not agree well with the measurements. The turbulence treatment near the wall is very important and wall functions are not suitable.

Dhiman and A.K (28), investigated the flow and heat transfer characteristics of an isolated square cylinder in crossflow placed symmetrically in a planar slit for a range of conditions. They obtained the heat transfer correlations in the steady flow regime for the constant temperature and constant heat flux boundary conditions on the solid square cylinder in crossflow. In addition, variation of the local Nusselt number on each face of the obstacle and representative isotherm plots are presented to elucidate the role of Prandtl number and blockage ratio on drag coefficient and heat transfer

Cheng and Yal. (29) numerically investigated the fluid flow and heat transfer characteristics of mixed convection in three-dimensional rectangular channel with four heat sources. The SIMPLEC algorithm was applied to deal with the coupling between pressure and velocity, and new high-order stability guaranteed second-order difference (SGSD) scheme was adopted to discretize the convection term. They studied the influence of four parameters: Richardson number, heat source distribution, channel height and inclination angle. They analyzed the numerical results from the viewpoint of the field synergy principle, which says that the enhanced convective heat transfer is related not only to the velocity field and temperature field, but also to the synergy between them. They found that the effects of the four parameters on the thermal performance can all be explained with the field synergy principle. To obtain better electronic cooling, the synergy between the velocity and temperature gradient should be increased when other conditions are unchanged.

Kumara and Setal. (30) investigated the complex unsteady flow through and around a channel in the presence of an obstruction at the entry is studied by solving directly the unsteady Navier–Stokes equations. They considered the Reynolds number of 4000, as experimental results are available for comparison. The computed results are in close

agreement with experiments. The computations help with better understanding of the phenomenon of reverse flow and fluid pumping.

Roy and Aet (31) conducted a similar type investigation by developing a fully explicit two-dimensional incompressible laminar Navier-Stokes solver in primitive variable formulation using a Cartesian staggered grid. The governing flow equations have been solved on the physical plane using a finite volume discretisation scheme. They discretized the convective terms of the solver using the weighted second upwind SOLA scheme. The pressure is solved by using the SOLA pressure correction algorithm. The diffusive terms of the momentum equations are discretised by using central differencing scheme. In their investigation, flow past a square cylinder placed inside a channel with two different blockage ratios, namely, 0.125 and 0.250 have been computed at four different Reynolds numbers, namely, 150, 300, 750 and 1500. The average drag coefficient increases with an increase in blockage ratio for a given Reynolds number. The vortex shedding frequency also increases with increase in blockage ratio. Recirculation zones are formed on the channel wall surfaces for Reynolds numbers 750 and 1500, respectively. Recirculating zones on the walls are affected by the vortex shedding process. Their structure and location get modified from time to time. Streamlines, vorticity contours and pressure contours are provided to analyze the important characteristics of the flow field. The results compare well with those available from literature.

Rodgers (32), assessed the numerical predictive accuracy for component-printed circuit board (PCB) heat transfer in forced convection using a widely used computational fluid dynamics (CFD) software, as component junction temperature prediction accuracy for the populated board case is typically within 65°C or 610%, which would not be sufficient for temperature predictions to be used as boundary conditions for subsequent reliability and electrical performance analyses. Neither the laminar nor turbulent flow model resolves the complete flow field, suggesting the need for a turbulence model capable of modeling transition. They show that the full complexity of component thermal interaction is not to be fully captured.

Heat transfer phenomenon in micro-channel heat sinks using three-dimensional numerical analysis was investigated by Weilin Qu (33) and Ryu (34).This paper presents the

three-dimensional fluid flow and heat transfer in a rectangular microchannel heat sink are analyzed numerically using water as the cooling fluid. The heat sink consists of a 1-cm^2 silicon water. The microchannels have a width of 57μm and a depth of 180μm, and are separated by a 43 μm wall. A numerical code based on the finite difference method and the SIMPLE algorithm is developed to solve the governing equations. By investigation it is found that the temperature rise along the flow direction in the solid and fluid regions can be approximated as linear. The highest temperature is encountered at the heated base surface of the heat sink immediately above the channel outlet. The heat flux and Nusselt number have much higher values near the channel inlet and vary around the channel periphery, approaching zero in the corners. For a relatively high Reynolds number of 1400, fully developed flow may not be achieved inside the heat sink. Increasing the thermal conductivity of the solid substrate reduces the temperature at the heated base surface of the heat sink, especially near the channel outlet.

Hetsroni (35) & (36) analyzed the effect of geometry on flow and heat transfer, finding that an increasingly uniform heat flux resulted in an increased irregularity of temperature distribution on the chip surface.

Analysis of two-layered microchannel heat sink concept in electronic cooling was proposed by Kambiz (37) this work shows a new concept for a two-layered microchannel heat sink with counter current flow arrangement for cooling of the electronic components is proposed. The thermal performance and temperature distribution for these types microchannels were analyzed and a procedure of optimizing the geometrical design parameters is presented the streamwise temperature rise on the base surface was found to be substantially reduced compared to that of the one-layered heat sink. At the same time the pressure drop required for the two-layered heat sink was found to be substantially smaller than that of the one-layered heat sink. The results demonstrate that the two-layered microchannel heat sink design is a substantial improvement over the conventional one-layerd microchannel heat sink. This study is focused on the temperature distribution, thermal resistance and the optimization of geometrical design parameters.

Numerical and Experimental Investigation of Micro-channel Heat sinks for cooling Electronic Devices was numerically studied by Lior (38). FLUENT, a computational fluid dynamics (CFD) program was used to predict the temperature distribution in a micro-channel

heat exchanger. The results from the numerical simulation were then compared to experimental data. The experimental data was gathered by monitoring a single 0.31mm x 10mm cross-section micro-channel chip that was cooled using water flow convection. The chip was heated by applying voltage to an aluminum heater, and temperatures from 40^0 C to 120^0 C were observed using an infrared camera, it has been determined that higher flow rate is better for convection. The results also demonstrated that an increase in the use of a high mass flux improves single-phase convection flow. The experiment illustrated that the thermal resistance is independent of the heat flux values.

2.5 Experimental studies

Li and Ewoldt (39) evaluated experimentally the effect of altitude on electronic cooling . As material properties of air vary as a function of altitude due to changes in atmospheric pressure and temperature. These changes have a negative impact on the heat transfer effectiveness and result in higher component temperature when compared to sea level conditions. They carried out the experiments in a hypobaric chamber using electronic printed circuit boards populated with heated rectangular blocks placed in a small wind tunnel. The altitude was varied between 0 and 5000 m above sea level and the air speed is varied between 1 and 5 m/s. The results show the local adiabatic heat transfer coefficient and thermal wake function diminish with altitude. This information is useful for design and analysis of electronic equipment for operation over a range of altitudes and air speeds typically encountered in forced air convection cooling applications.

Haider (39) studied a model for the two-phase flow and heat transfer in the closed loop, two-phase thermosyphon (CLTPT) involving co-current natural circulation. The focus was on CLTPTs for electronics cooling that exhibit complex two-phase flow patterns due to the closed loop geometry and small tube size. They used homogeneous two-phase flow model to evaluate the

Friction pressure drop of the two-phase flow imposed by the available gravitational head through the loop. They used the boiling characteristics of the enhanced structure to predict the chip temperature. The comparison with experimental data for dielectric working fluid PF-5060 and was in general agreement with the observed trends.

Yoo(40) investigated how the flow via an obstruction in forced convection influence the local heat transfer from electronic modules. They have conducted experiments on a three-dimensional array of hexahedral elements as well as on a two-dimensional array of rectangular elements. Naphthalene sublimation technique was employed to measure three-dimensional local mass transfer, and the mass transfer data are converted to their counterparts of the heat transfer process using the analogy equation between heat and mass transfer. Module location and stream wise module spacing were varied, and the effect of vortex generators on heat transfer enhancement was also examined. The results show dramatic change of local heat transfer coefficients on each surface of the module, and three-dimensional modules have a little higher heat transfer value than two-dimensional modules because of bypass flow. Longitudinal vortices formed by vortex generator enhance the mixing of fluids and thereby heat transfer, and the rectangular wing type vortex generator is found to be more effective than the delta wing type vortex generator.

Tae hoji (41) performed experiments to investigate heat dissipation from a heated square cylinder in a channel by oscillating flow. During the experiments, the input power and oscillating amplitude (A) were fixed. The effects of the Reynolds number based on the mean flow velocity and the oscillating frequency on the heat transfer enhancement are examined. They determined the time averaged Nusselt number and the Strouhal number for each oscillating condition. The measured Strouhal numbers according to the Reynolds number are compared with the previous results and good agreement is found. The occurrence of the "lock-on" phenomenon is demonstrated for a square cylinder. When the pulsating frequency is in the lock-on regime, the heat transfer from a square cylinder is dramatically enhanced. They found that the heat transfer enhancement is pronounced as the Reynolds number increases.

(42) estimated experimentally the continuous, one-dimensional kernel function in a rectangular duct subject to forced convection with air using liquid crystal thermography techniques. They manipulated the Analytical relationships between the kernel function for internal flow and the temperature distribution resulting from a known heat flux distribution to accomplish this objective.

They proposed a model for the kernel function in the hydrodynamic entry region of the rectangular duct, and used in its experimental determination. The kernel functions

obtained by the work were shown to be capable of predicting the highly non uniform surface temperature rise above the inlet temperature resulting from an arbitrary heat flux distribution to within the experimental uncertainty. This is better than the prediction obtained using the analytically derived kernel function for turbulent flow between parallel plates, and the prediction obtained using the conventional heat transfer coefficient for constant heat flux boundary conditions. The latter prediction fails to capture both the quantitative and qualitative nature of the problem. The results of their work are relevant to applications involving the thermal management of non uniform temperature surfaces subject to internal convection with air, such as board level electronics cooling.

De and Voe (43) performed a systematic study of the influence of board conduction on the predictive accuracy of Compact Thermal Models of BGA and CPGA package styles. Various resistance network topologies were assessed by them for each package style. They created the detailed (FE) isotropic board models with conductivities spanning three orders of magnitude to test the influence of board conductivity on CTM accuracy. They compared the results to equivalent fully-detailed (FE) package models on detailed board models. The predictive capability of the optimized topologies was strongly correlated to the existence of strong local temperature gradients in the board, whenever the sensitivity to board heat conduction was high. When the board is poorly conducting (k=l W/m-K), board heat conduction is too low to matter. When the board is highly conducting (k= l00 W/m-K), the high conductivity smoothes out local board temperature gradients, and the CTMs are accurate even though the board heat flow path is dominant. In general, they found that optimized network topologies that included shunt resistances to predict the junction temperature to within 5% to 8% over a wide range of board conductivities, while star-shaped networks were generally only accurate to 10-15 %.

Following the work of Tuckerman and Pease , many studies have been performed to characterize flow and heat transfer in microchannel structures. Friction factor Nusselt number are the two primary parameters examined in most of the experimental literature. Several studies indicated that these two parameters deviate from the classical theory developed for macro-size channels and the transition from laminar to turbulent flow occurs at a smaller critical Reynolds number. Unfortunately there is no consensus on the trend of this deviation among different researchers. For instance, Wu and Little tests for flow of gas in trapezoidal

microchannels and the found the friction factor for laminar flow in microchannel to be generally larger than predicted by the Moody diagram and to be affected by surface roughness. Fahler and Gerner (44) however found the friction factor for microchannels to be smaller than predicted by laminar theory.

In typical flow experiments, the pressure drop was measured across plenums at the end of micro channel. This bulk property is usually lumped with other hydraulic losses such as header loss, entrance effects and uncertainties due to various factors mentioned in the previous research work. This made it difficult to interpret the experimental data and to compare results among different researchers.

The single phase forced convective heat transfer and flow characteristics of water in micro channel structures/plates with small rectangular channel hydraulic diameters of 0.133-0.367 mm and distinct geometric configurations were investigated experimentally by Peng , X. F. and G. P. Peterson . The laminar heat transfer was found to be dependent upon the aspect ratio and the ratio of hydraulic diameter to the center-center distance microchannel. The flow resistance of the liquid flow in the microstructures was also investigated experimentally and analytically, and correlations were proposed for the calculation of the flow resistance

Experimental investigation on liquid forced convection heat transfer through microchannels was studied by B. X. Wang .The experiments were conducted to investigate the single phase forced flow convection of water methanol flowing through microchannels with rectangular cross-section. The transition and laminar heat transfer behavior on microchannels are very unusual and complex and are strongly affected by liquid temperature, velocity and microchannel size.

2.6 Closure

Many research papers were published regarding electronics chip cooling. Some of them investigated analytically, some are numerically and rest experimentally predicted. The

implementation of this technology is still in its infancy. Major obstacles in implementing this technology are due to the lack of substantial understanding in the behavior of microchannel system. There are many challenges in microchannel fluid mechanics and heat transfer study. Therefore, scientific approach in analyzing the fluid flow and heat transfer behavior in microchannel is essential in developing a viable cooling solution. Mostly analytical solutions are newly developed techniques which needs validations. Numerical solutions are, solving the governing equations by different techniques, or using the commercially available codes. But validating the codes is also an ongoing process, which is still going on. And finally the experimental investigation results are practically needed results. So the experimental results are also required to validate the CFD codes and analytical results. In this study we will solve the governing equations by SIMPLE method and analyze the results obtained.

CHAPTER 3

Mathematical Formulation

- Ø ***Introduction***
- Ø ***Governing Equations***
- Ø ***Boundary Conditions***
- Ø ***Background Of Theory***
- Ø ***Computational Fluid Dynamics & FLUENT***
- Ø ***Gambit steps &fluent steps***
- Ø ***Closure***

3.1 Introduction

Here the micro-heat sink model consists of a 10 mm long substrate and dimension of rectangular microchannels have a width of 57 µm and a depth of 180 µm as shown in Fig (3.1). The heat sink is made from silicon and water is used as the cooling fluid. The electronic component is idealized as a constant heat flux boundary condition at the heat sink bottom wall. Heat transport in the unit cell is a conjugate problem which combines heat conduction in the solid and convective heat transfer to the coolant (water).Here we consider a rectangular channel of dimension (900µx100µmx10mm) applied constant heat flux of 90W/cm^2 from bottom as given table(1). Water flowing through channel at temperature 293k on account of pressure loss of 50kpa the model in this study uses a unit grid dimension of 99X90X10 as in Fig (3.2).

Here we assumed to have a constant heat flux, *q*"(90W/cm^2)at the bottom wall .The other wall boundaries of the solid region are assumed perfectly Insulated with zero heat flux. The water flow velocities are taken from different Reynolds numbers, from 96 to 164, with reference to the hydraulic diameter of 86 µm.

3.1.1 Description Of The Designed Cooling Model

Here the micro-heat sink model consists of a 10 mm long substrate and dimension of rectangular microchannels have a width of 57 µm and a depth of 180 µm and we consider a rectangular channel of dimension (900µx100µmx10mm) applied constant heat flux of 90W/cm^2 from bottom as Fig (2)

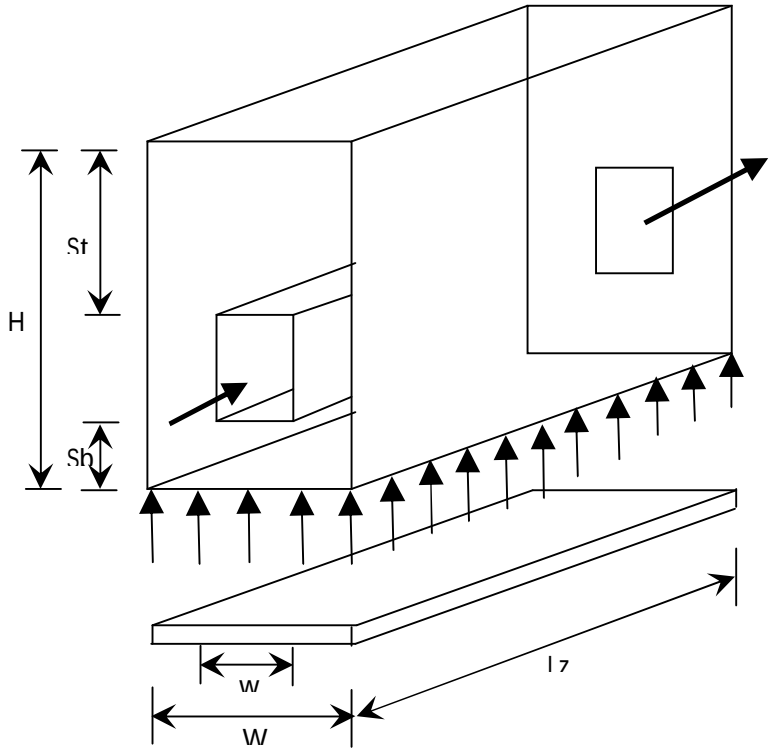
H
St
Sh
w
W

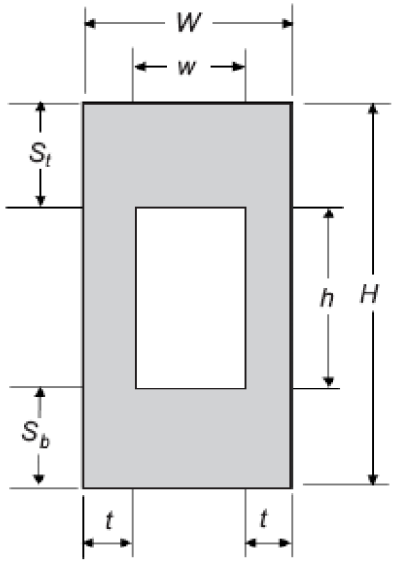
W
w
S_t
h
H
S_b
t
t

W	w	H	h	t	St	Sb	Lz	Dh
100µm	57µm	100µm	180µm	21.5µm	450µm	270µm	10000µm	86.58

Fig-(3.1) Geometric dimensions of single channel

3.1.2 Assumptions

.

Laminar flow.

Uniform wall heat flux.

Negligible radiation heat transfer

Constant heat flux $9x10^5$

Incompressible fluid

Variable thermophysical properties

In this chapter the fundamental governing equations are continuity, momentum and energy equations which are derived from basic principles of heat and fluid flow. The equations are posed to implement SIMPLE (Semi-Implicit Method for Pressure Linked equation) algorithm. Consequently the Navier-Stoke's equations are solved.

3.2 Governing Equations

The conjugate heat transfer and the fluid flow inside the microchannel structure were numerically modeled. Steady state continuity, momentum (Navier-stokes Equation) and energy equations are solved. Laminar incompressible flow assumed.-

3.2.1 Continuity Equation

$$\frac{\partial u}{\partial x}+\frac{\partial v}{\partial y}+\frac{\partial w}{\partial z}=0 \qquad \text{.....[1]}$$

3.2.2 Momentum equation

Let (x, y, z) be the orthogonal components of the body force field in the Cartesian coordinate system; then

$$\rho\left(u\frac{\partial u}{\partial x}+v\frac{\partial u}{\partial y}+w\frac{\partial u}{\partial z}\right) = -\frac{dp}{dx}+\mu\left(\frac{\partial^2 u}{\partial x^2}+\frac{\partial^2 u}{\partial y^2}+\frac{\partial^2 u}{\partial z^2}\right) \text{.....[2]}$$

3.2.3 Energy Equation

$$\left(u\frac{\partial T}{\partial X}+v\frac{\partial T}{\partial Y}+w\frac{\partial T}{\partial Z}\right)=\frac{1}{\alpha}\left(\frac{\partial^2 T}{\partial X^2}+\frac{\partial^2 T}{\partial y^2}+\frac{\partial^2 T}{\partial Z^2}\right) \qquad \text{.....[3]}$$

3.3 Boundary conditions

3.3.1 For the hydraulic boundary conditions, the velocity is zero at all boundaries except the channel inlet and outlet. A uniform velocity is applied at the channel inlet.i.e.

At inlet x=0 $p=p_1$, v=0, w=0

At outlet x=Lx $p=p_0$, v=0, w=0

At inner wall surface no slip condition (u=0,v=0,w=0)

3.3.2 For thermal boundary conditions, adiabatic boundary conditions are applied to all the boundaries of the solid region except the channel inlet, channel outlet and heat sink bottom wall, where a constant heat flux is applied.

At the channel inlet, the liquid temperature is equal to a given constant inlet temperature i.e. T=Tin for x=0 and

At $y=0,\ -k_w\frac{\partial T_w}{\partial y}=q''$ (3.14)

At $y=H,\ -k_w\frac{\partial T_w}{\partial y}=0$ (3.15)

At $z=0$, if (y, x)$\in$ channel $T_f=T_{fi}$

Or $-k_w\frac{\partial T_w}{\partial z}=0$ (3.16)

At $z=L$, if (y, x)$\in$ channel $-k_f\frac{\partial T_f}{\partial z}=0$

Or $-k_w\frac{\partial T_w}{\partial z}=0$ (3.17)

At $x=0,\ -k_w\frac{\partial T_w}{\partial x}=0$

Or $x=w,\ -k_w\frac{\partial T_w}{\partial x}=0$ (3.18)

3.3 Background of Theory

Heat is defined as energy transferred by virtue of temperature difference or gradient. Being a vector quantity, it flows with a negative temperature gradient. In the subject of heat transfer, it is the rate of heat transfer that becomes the prime focus. The transfer process indicates the tendency of a system to proceed towards equilibrium. There are 3 distinct modes in which heat transfer takes place:

3.4.1 Heat transfer by Conduction:

Conduction is the transfer of heat between 2 bodies or 2 parts of the same body through molecules. This type of heat transfer is governed by Fourier`s Law which states that – "Rate of heat transfer is linearly proportional to the temperature gradient". For 1-D heat conduction-

$$q_k = -k\frac{dT}{dx}$$

3.4.2Heat transfer by Convection:

When heat transfer takes place between a solid surface and a fluid system in motion, the process is known as Convection. When a temperature difference produces a density difference that results in mass movement, the process is called Free or Natural Convection.

When the mass motion of the fluid is carried by an external device like pump, blower or fan, the process is called Forced Convection. In convective heat transfer, Heat flux is given by:

$$q(x) = h_x(T_w - T_\infty)$$

3.4.3Reynold`s Number**:**

It is the ratio of inertial forces to the viscous forces. It is used to identify different flow regimes such as Laminar or Turbulent.

$$R_e = \frac{\rho VD}{\mu} = \frac{VD}{\nu} = \frac{Inertial\ Forces}{Viscous\ Forces}$$

3.4.4 Nusselt Number**:-**

The Nusselt number is a dimensionless number that measures the enhancement of heat transfer from a surface that occurs in a real situation compared to the heat transferred if just conduction occurred.

$$Nu_L = \frac{hL}{k_f}$$

3.4.5 Prandtl Number:-

It is the ratio of momentum diffusivity (viscosity) and thermal diffusivity.

$$\Pr = \frac{\nu}{\alpha}$$

3.4.5 Grashof Number:-

It is the ratio of Buoyancy force to the viscous force acting on a fluid.

$$Gr = \frac{g\beta\ (T_s - T_\infty)L^3}{\nu^2}$$

3.4.6 Rayleigh Number:-

It is the product of Grashof number and Prandtl number. It is a dimensionless number that is associated with buoyancy driven flow i.e. Free or Natural Convection. When the Rayleigh number is below the critical value for that fluid, heat transfer is primarily in the form of conduction; when it exceeds the critical value, heat transfer is primarily in the form of convection.

$$\mathrm{Ra}_x = \mathrm{Gr}_x \mathrm{Pr} = \frac{g\beta}{\nu\alpha}(T_s - T_\infty)x^3$$

3.4.7 Solution Approaches:-

Step1 Pressure inlet is calculated by putting values of eq (3.24),(3.25),(3.26)

$$\Delta P = f \frac{4L_X}{D_h}\left(\frac{1}{2}\rho u_m^2\right) \quad (3.23)$$

Step2 Friction factor is calculated

$$f = \frac{H^2 + W^2}{(H+W)^2}\frac{24}{\mathrm{Re}_{Dh}} \quad (3.24)$$

Step3 Reynolds Number is obtained

$$\mathrm{Re}_{Dh} = \rho VD/\nu \quad (3.25)$$

Step 4 Hydraulic Diameter is calculated

$$D_h = \frac{4A_w}{\Gamma} = \frac{4HW}{2(H+W)} \quad (3.26)$$

Step5 Velocity is obtained and then mass flow rate

$$\dot{m} = \rho_f . u_m . A_w$$

16. Relaxation factors are follows:-

Pressure = 0.3

Density = 1

Momentum = 0.7

Body forces = 1

3.4 COMPUTATIONAL FLUID DYNAMICS (CFD) & FLUENT

Computational fluid dynamics (CFD) is one of the branches of fluid mechanics that uses numerical methods and algorithms to solve and analyze problems that involve fluid flows. The numerical solver codes are well-established and thus provide a good start to more complex heat transfer and fluid flow problems. FLUENT provides adaptability to variation of thermo physical properties with respect to temperature effect. The fundamental basis of any CFD problem is the Navier-Stokes equations, which define any single-phase fluid flow.

These equations can be simplified by removing terms describing viscosity to yield the Euler equations. Further simplification, by removing terms describing vorticity yields the full potential equations. Finally, these equations can be linearized to yield the linearized potential equations.

The single layer micro channel is simulated to compare the results with available numerically simulated results by J. Li et al[11].GAMBIT is a physical domain creation and discretization (meshing) soft ware, which is easily detected by 3-D FLUENT solver interface. The interior micro channel is meshed with double spacing technique as shown in Figure below. Then the 2-D face is generated by mapping technique. The 3-D meshing is done by extruding of grid generation.

The stability of the chosen discretization is generally established numerically rather than analytically as with simple linear problems. Special care must also be taken to ensure that the discretization handles discontinuous solutions gracefully. The Euler equations aı Navier-Stokes equations both admit shocks, and contact surfaces. Some of the discretization methods being used are:

3.5.1FINITE VOLUME METHOD**:-**

This is the "classical" or standard approach used most often in commercial software and research codes. The governing equations are solved on discrete control volumes. This integral approach yields a method that is inherently conservative (i.e., quantities such as density remain physically meaningful)

$$\frac{\partial}{\partial t}\iiint Q dV + \iint F d\mathbf{A} = 0$$

Where Q is the vector of conserved variables, F is the vector of fluxes (see Euler equations or Navier-Stokes equations), V is the cell volume, and is the cell surface area.

3.5.2FINITE ELEMENT METHOD**:-**

This method is popular for structural analysis of solids, but is also applicable to fluids. The FEM formulation requires, however, special care to ensure a conservative solution. The FEM formulation has been adapted for use with the Navier-Stokes equations. In this method, a weighted residual equation is formed:

$$R_i = \iiint W_i Q dV^e$$

Where Ri is the equation residual at an element vertex i , Q is the conservation equation expressed on an element basis, Wi is the weight factor and Ve- is the volume of the element.

3.5.3FINITE DIFFERENCE METHOD**:-**

This method has historical importance and is simple to program. It is currently only used in few specialized codes. Modern finite difference codes make use of an embedded boundary for handling complex geometries making these codes highly efficient and accurate. Other ways to handle geometries are using overlapping-grids, where the solution is interpolated across each grid.

$$\frac{\partial Q}{\partial t} + \frac{\partial F}{\partial x} + \frac{\partial G}{\partial y} + \frac{\partial H}{\partial z} = 0$$

Where Q is the vector of conserved variables, and F, G, and H are the fluxes in the x, y, and z directions respectively.

3.6 Schemes to Calculate Face Value for variables:-

3.6.1 Central Difference scheme:

This scheme assumes that the convective property at the interface is the average of the values of its adjacent interfaces.

3.6.2 The UPWIND scheme:

According to the upwind scheme, the value of the convective property at the interface is equal to the value at the grid point on the upwind side of the face. It has got 3 sub-schemes i.e. 1^{st} order upwind which is a 1^{st} order accurate, 2^{nd} order upwind which is 2^{nd} order accurate scheme and QUICK (Quadratic Upwind Interpolation for convective kinematics) which is a 3^{rd} order accurate scheme.

3.6.3 The EXACT solution:

According to this scheme, in the limit of zero Peclet number, pure diffusion or conduction problem is achieved and φ vs x variation is linear. For positive values of P, the value of φ is influenced by the upstream value. For large positive values, the value of φ seems to be very close to the upstream value.

3.6.4 The EXPONENTIAL scheme

When this scheme is used, it produces exact solution for any value of Peclet number and for any value of grid points. It is not widely used because exponentials are expensive to compute.

3.6.5 The HYBRID scheme

The significance of hybrid scheme can be understood from the fact that (i) it is identical with the Central Difference scheme for the range -2<=Pe<=2 (ii) outside, it reduces to the upwind scheme

3.7GAMBIT AND FLUENT STEPS

3.7.1 Gambit steps

STEP 1 Select a solver:

Main Menu>Solver>Fluent 5/6.

STEP 2 Creation of Vertices:

Operation>Geometry>Vertex Command Button>Create Vertex from Co-ordinates.

The following vertices with the required Cartesian co-ordinates were created. All dimensions are in 'µm'

Vertices	Cartesian Co-ordinates
A	-50,-450,0
B	50,-450,0
C	50,450,0
D	-50,450,0
P	-28.5,0,0
Q	-28.5,-180,0
R	28.5,-180,0
S	28.5,0,0
0	50,-450,10000

STEP 3 Creation of Line:

Operation>Geometry>Creating Edge>Straight.

Create straight lines by joining the following vertices AB,BC,CD,DA,PQ,QR,RS,SP,DO.

STEP 4 Creation of Faces:

Operation>Geometry>Face Command Button>Form Face>Create Face from Wireframe.

To create face 'ABCD', select edges in a sequence order (AB>BC>CD>DA) and click apply. Similarly, create PQRS using the same above commands.

STEP 5 Meshing Edges (PQ, QR, RS, SP):

(a) Operation>Mesh>Mesh edges.

Select Edge-PQ,RS

Grading-Apply

Type-Successive ratio.

Ratio-1.05 (Double sided)

Spacing-Apply

Interval Count- 90

Mesh-Apply

Click Apply.

(b) Select edge- QR, SP

Grading-Apply.

Type-Successive Ratio.

Ratio-1.05 (Double sided)

Spacing-Apply

Interval Count-28

Mesh-Apply

Click Apply.

STEP 6 Subtract faces.

Operation>Geometry>Face Command Button>Boolean operations>Subtract.

Subtract face PQRS from ABCD.

STEP 7 Mesh face.

Operation>Mesh Command Button>Face mesh>Mesh faces.

Faces- Select face 1

Elements- Quad.

Type- Pave

Interval Size- 2

STEP 8 Face Creation and meshing.

Again, create a face PQRS by joining the sides PQ, QR, RS, SR.

Mesh PQRS by following the above meshing method with an interval size of 2. The scheme should be Pave mesh.

STEP 9 Meshing Edge DO:

Operation>Mesh>Mesh Edges.

Select Edge-BH

Grading-Apply

Type-Successive ratio.

Ratio-1

Spacing-Apply

Interval Count-20

Mesh-Apply

Click Apply

STEP 10 Creation of Volume:

Operation>Geometry>Volume>Form Volume>Sweep Real Faces.

Select all the faces.

Path-Edge.

Edge-Select Line DO with mesh.

Click Apply.

STEP 11 Creating Zones.

Operation>Zones Command Button>Specify Boundary Types.

Name	Type
Inlet sink	Wall
Channel inlet	Mass flow inlet
Heat flux	Wall
Base channel	Wall
Channel right	Wall
Channel left	Wall
Sink right	Wall
Channel top	Wall
Sink left	Wall
Sink top	Wall
Sink outlet	Wall
Channel outlet	Outflow

STEP 12 Creation of Continuum.

Operation>Zones Command Button>Specify Continuum Types.

59

Name	Type
Heat sink	Solid
Channel	Liquid

STEP 13 File>Save as [name]

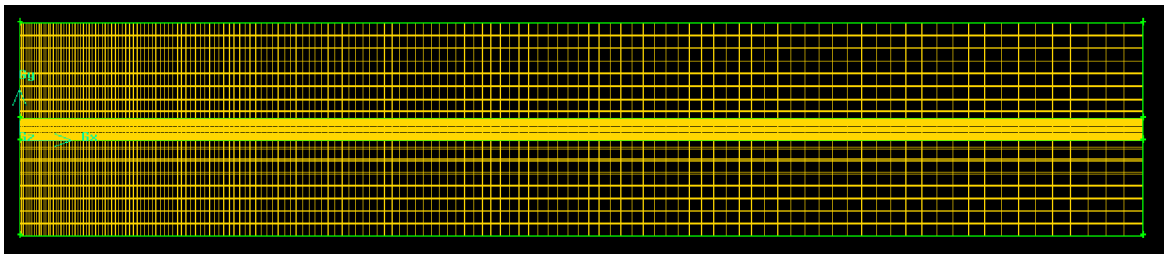

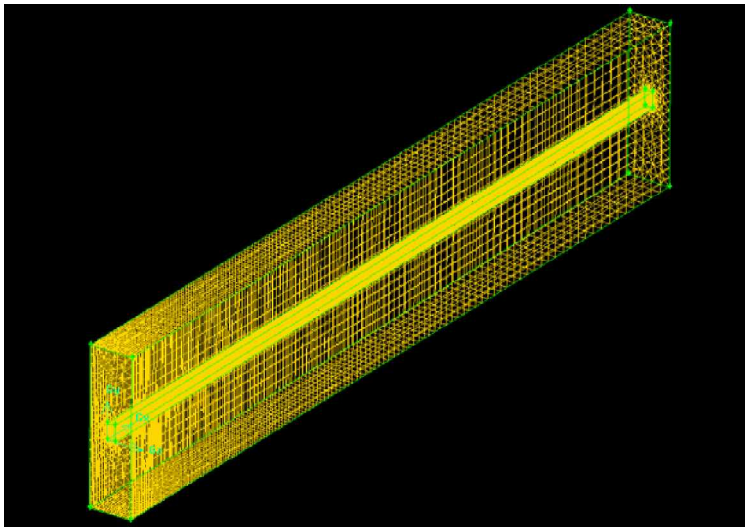

Fig (3.2) Microchannel model: (a) side view; (b) model view.

STEP 14 File>export>Mesh[File name]

3.7.2 FLUENT STEPS:-

STEP 15 Select FLUENT 3ddp.

STEP 16 Reading of the mesh file.

File>Read>Case.

STEP 17 ANALYSIS OF GRID.

a) Checking of grid

Grid>Check.

It was checked that the total volume doesn't come as negative.

b) Scaling of Grid.

Grid>Scale.

Scale was set to 1e-6 in X, Y, Z directions.

c) Smoothing and Swapping.

Grid>Smooth/swap.

The grid was swapped until Zero faces were moved.

STEP 18 SELECTION OF MODELS.

(a) Defining solver.

DEFINE>MODELS>SOLVER.

Solver is segregated

Implicit formulation

Space steady

Time steady

(b) Define Energy Equation.

DEFINE > MODEL >ENERGY.

(c) Selection of Materials.

Fluid was taken to be liquid water which was selected from the fluent database with variable properties.

Solid was changed to SILICON whose properties were:

Density, = 2330 Kg/m^3.

Specific Heat Capacity, k= 714 J/Kg/°C.

Thermal Conductivity, C_p= 140

(d)Defining Operating Conditions.

STEP19 DEFINE > OPERATING CONDITIONS.

Operating pressure= 101.325 KPa

Gravity = -9.81 m/s2 in Y-direction

STEP20 DEFINE >BOUNDARY CONDITIONS

Channel Inlet.

Input the following values at Mass Flow Inlet.

Mass Flow Rate- 1e-5 kg/sec

Temperature- 293 K

Component of X and Y velocity Direction- 0

Component of Z velocity Direction- 1

1. Heat Flux.

Input the following values at Wall.

Select Heat Flux from the list.

Heat Flux = 50/90/150 e4 W/m^2.

Thickness = 450e-6 m

Click on shell conduction.

2. Channel left.

Input the following values at Wall.

Select Heat Flux from the list.

Heat Flux = 0 W/m^2.

Thickness = 21.5e-6 m

Click on shell conduction

STEP 21SELECTION OF SOLUTION.

(b) Defining Solutions.

STEP 22 SOLVE > CONTROLS>SOLUTIONS

Flow and energy equations used.

Pressure-Velocity Coupling- SIMPLE.

Under relaxation factors:

Pressure= 0.3

Density= 1

Body Force= 1

Momentum= 0.08

Energy= 1

Discretization:

Pressure= Standard.

Momentum= 2nd order upwind.

Energy= 2nd order upwind.

(c) Initializing the Solution.

The Problem was computed taking the values from all zones.

(d) Defining Monitors.

STEP 23 SOLVE > MONITORS>RESIDUALS.

Plot option was clicked.

Plotting was done in window 1 with 1000 iterations.

Convergence criterion:

Continuity= 0.0001

X-velocity= 0.0001

Y-velocity= 0.0001

Z- Velocity= 0.0001

Energy= 1e-8.

(e) Iterating the solution.

STEP 24 SOLVE >ITERATE.

No. of iterations=500.

Iterate till the solution is converged

CLOSURE

The total grid number is 90000(i(x) x i(y) x i(z)=100x90x10) is for the domain in fig[3] . This size of a fine grid mesh for the y and z directions was chosen in order to properly resolve the velocity and viscous shear layers as in Fig[4], and to more accurately define the conjugate heat transfer at the boundary layer of the channel, thereby improving the temperature result. but along x direction we take comparative coarse discretization because the temperature gradients are small compared to the gradients occurring in other directions and process time as well as the memory storage required increases as the number of grid nodes is increased. Here we applied FLUENT's segregated solver which is an implicit solver.

The unknown value for a given variable is computed from a set of linear equations, each of which is written for a single cell in the domain. Under-Relaxation factors have direct impact on convergence. Generally default values are used, but if convergence problems occur, then these values are modified. Decreasing these factors gradually helps convergence. Using segregated solver approach, the governing equations are solved sequentially. Several methods like SIMPLE, SIMPLEC, SIMPLER and PISO are available for this purpose. In our calculations the most common one, SIMPLE method, is used In order to expedite the convergence Of the calculations, a line-by-line iteration and a Tri- Diagonal Matrix Algorithm (TDMA) method with a Thomas algorithm the upwind scheme is used for the convection term .Since the governing equations are non-linear), many iterations may be done before a Converged solution is obtained.

CHAPTER 4

Results and Discussions

- Ø ***Introduction***
- Ø ***Temperature contour***
- Ø ***Average Heat Transfer Coefficient***
- Ø ***Average Nusselt Number vs Reynolds number***
- Ø ***CONCLUSION***
- Ø ***closure***

4.1 Introduction

A series of numerical calculations have been conducted by fluent and the results are presented in order to show the effects of heat flux and mass flow rate on the temperature distribution in the microchannel heat sinks. The results are devoted to the local temperature distribution in micro-heat sinks, the average bulk characteristics of heat transfer, and further general discussion. Furthermore, in order to better compare the computational results obtained here with the experimental data available in the literature, the average overall Nusselt number is defined and analyzed with respect to the variations in the Reynolds number. Here the thermal properties of water were chosen at a reference temperature. Because the thermophysical properties are temperature dependent, particularly the liquid viscosity, the velocity and consequently the Reynolds numbers are different under the same pressure drop conditions.

As discussed previously, the thermophysical properties of the liquid are based upon the estimated liquid bulk temperature .For ΔP=50kpa and 90W/cm^2 variation in the reference temperature from 20^{0}C to 32 ^{0}C, changes the mean velocity from 1.12 to 1.38 m/s, and results in a corresponding change in the Reynolds number from 99 to 146.here reference temperature is taken 32^{0}C.

4.3 Température contour

The temperature of the liquid at the inlet is initially uniform (at 20 ^{0}C). The temperature Profiles shown is due to the assumption of hydrodynamic fully developed Flow .It is interesting to note that the temperature is highest at the channel corner. This is due to the low velocity of the flow and maximum temperature of fluid at exit of channel. The reference temperature for the thermophysical properties of water was chosen as $T_{reference}$ =Tin +Tout/2. The principal issues in heat sink design are the overall heat transfer performance for electronic cooling and the local temperature gradient for determining the thermal stress. While a number of investigations are currently underway to actually measure the temperature

and pressure gradients in these microchannels It is apparent here that the asymptote, average Nusselt number 4.1 lies between the values for a constant axial wall heat flux, 4.8, and a constant axial wall temperature, 4.0, for fully developed laminar flow in ducts, of rectangular cross-section with approximately (W: H = 1: 3). The silicon conducts more heat through the channel walls results temperature rise of water from 293K to 309K. From, this observation it is evident that the silicon material of heat sink is more useful and efficient to dissipate heat from the electronics chips. For prediction of fluid flow and thermal characteristics ,contour of temperature in the fluid at the inlet and outlet of channel is shown in Fig (4.2).

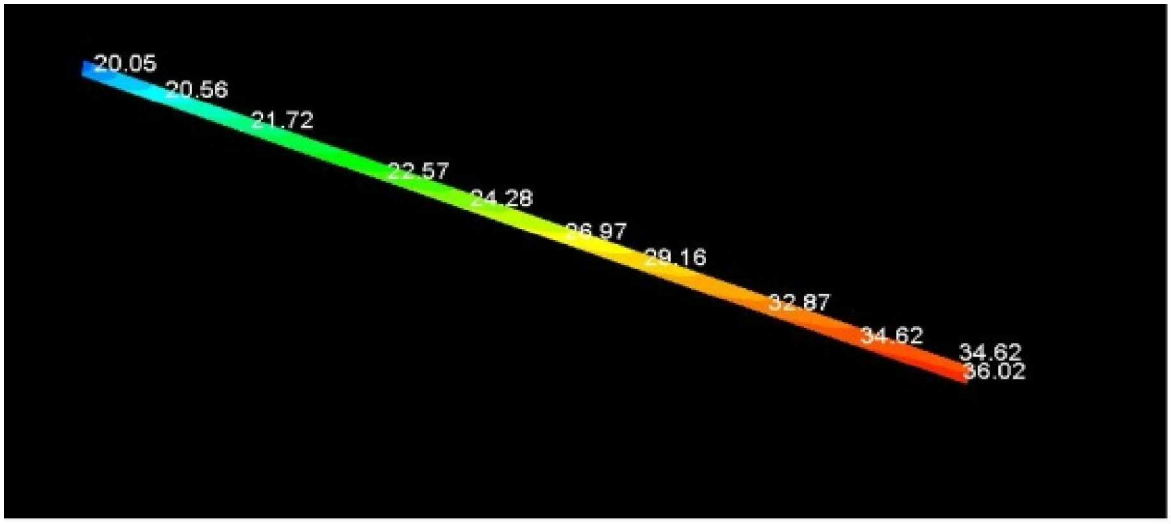

Fig-(4.1): local temperature distribution in X-Y plane at X=50μm for Δp=50 kpa and heat flux 90W/cm^2

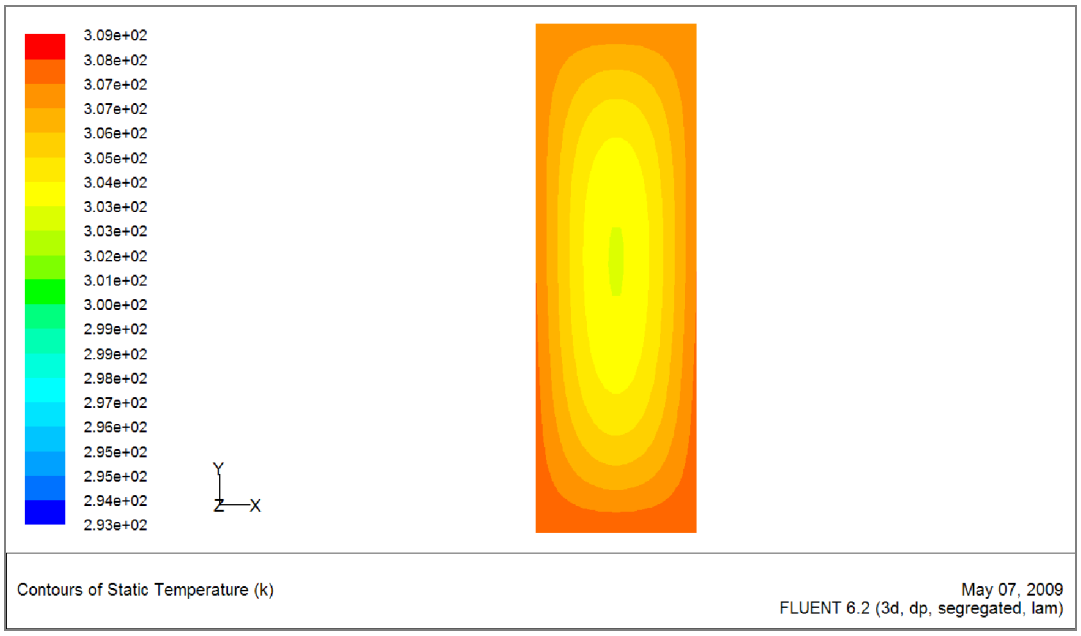

Fig (4.2):- Temperature contour of Silicon material at X = 50µm for Δp=50 kpa and heat flux 90W/cm^2 at outlet

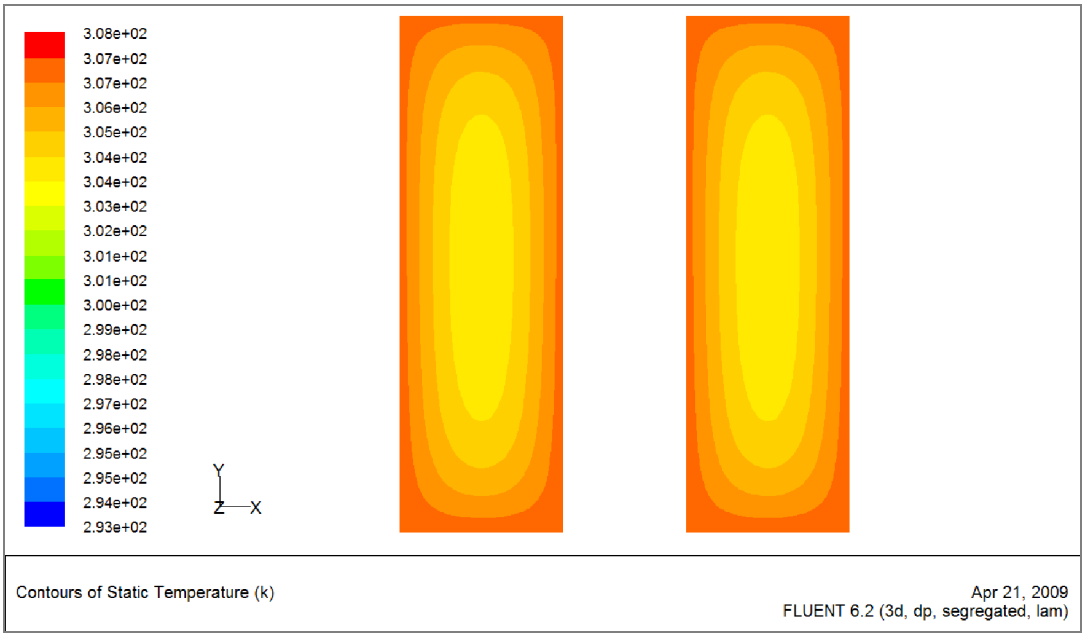

Fig. (4.3)Temperature of Outlet at Adiabatic wall conditions for double parallel channel

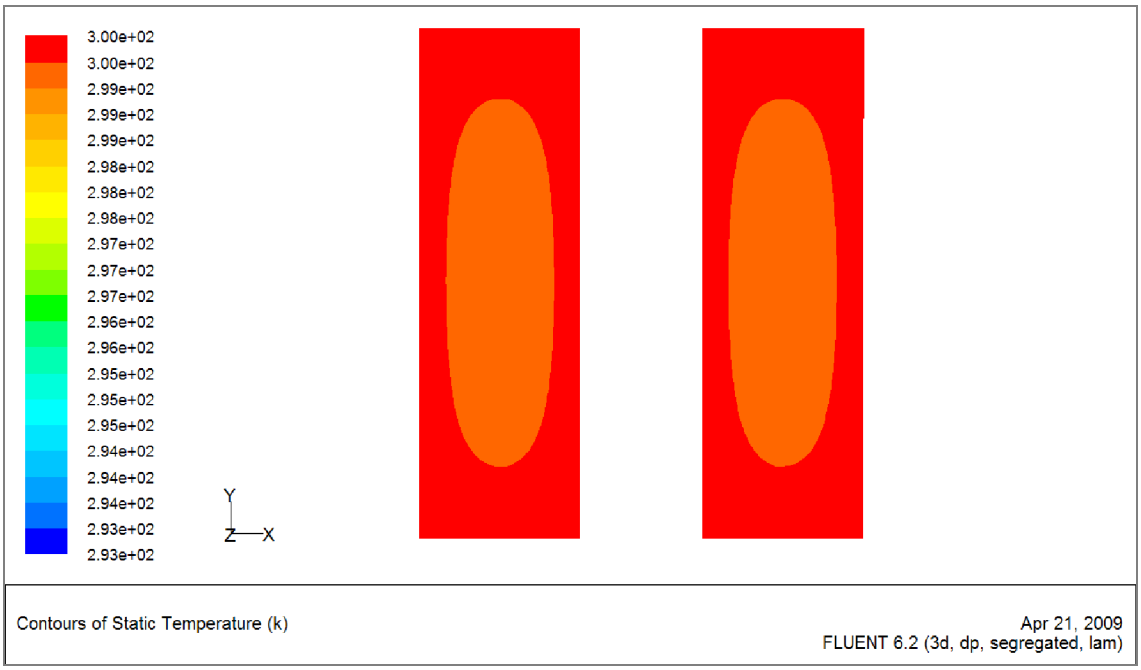

Fig. (4.4) Temperature contour at Isothermal (300k) wall condition for parallel channel

Here we consider the Pressure difference of 10kpa and heat flux of 90W/cm^2. It is evident from Fig (4.5) due to less Velocity the fluid get sufficient time to heat up so highest temperature obtained in this case.

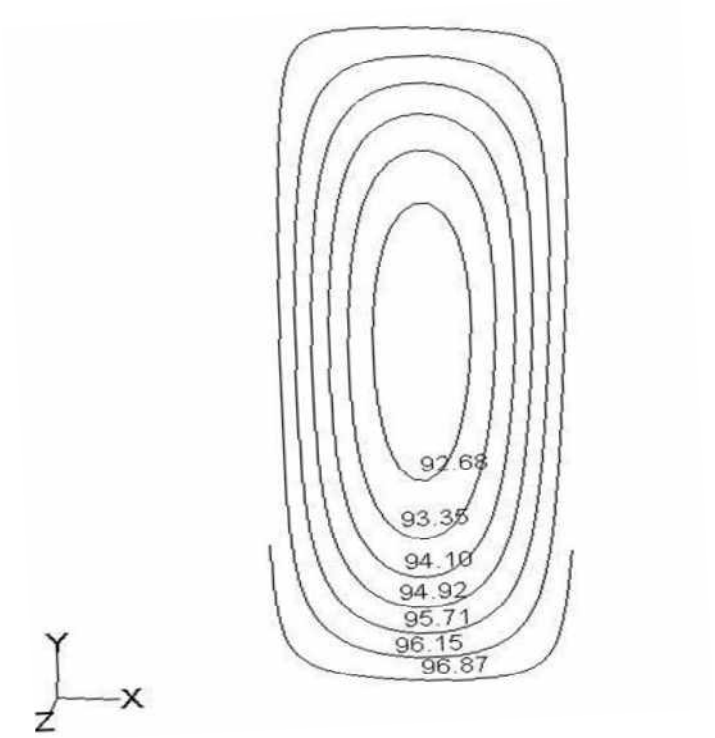

Fig(4.5):- Temperature contour of fluid at outlet for Pressure difference of 10kpa and heat flux of 90W/cm^2

Further we see pressure drop of 15 kpa and heat flux 90W/cm^2 and pressure drop of 50kpa and heat flux 90W/cm^2 Fig (4.6) and Fig (4.7).

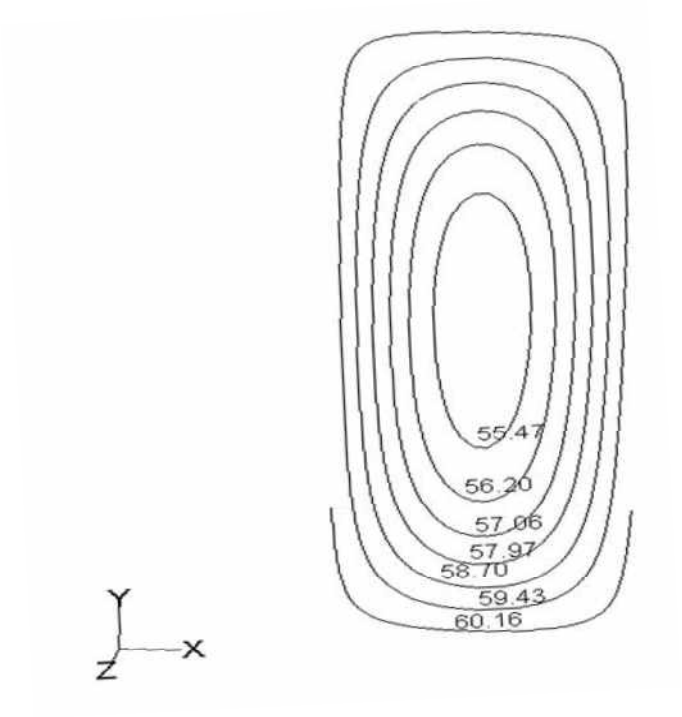

Fig (4.6):- Temperature contour of fluid at outlet for Pressure difference of 15 kpa and heat flux of 90W/cm^2

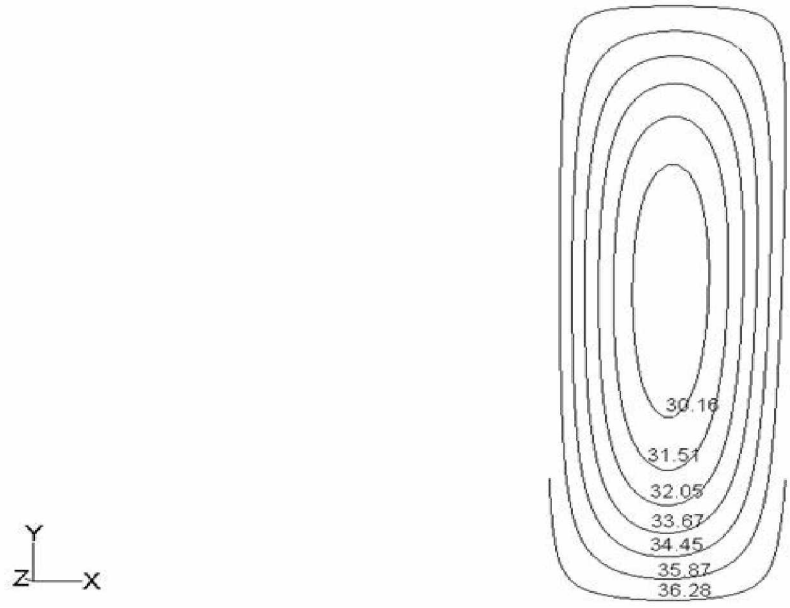

Fig (4.7):- Temperature contour of fluid at outlet for Pressure difference of 50kpa and heat flux of 90W/cm^2

For further analysis we take constant pressure drop of 50kpa but different heat flux of Magnitude 50W/cm^2, 90 W/cm^2 and 150W/cm^2 . The temperature contour of fluid is expressed in Fig 4.8 and Fig 4.9 and 4.10 respectively.

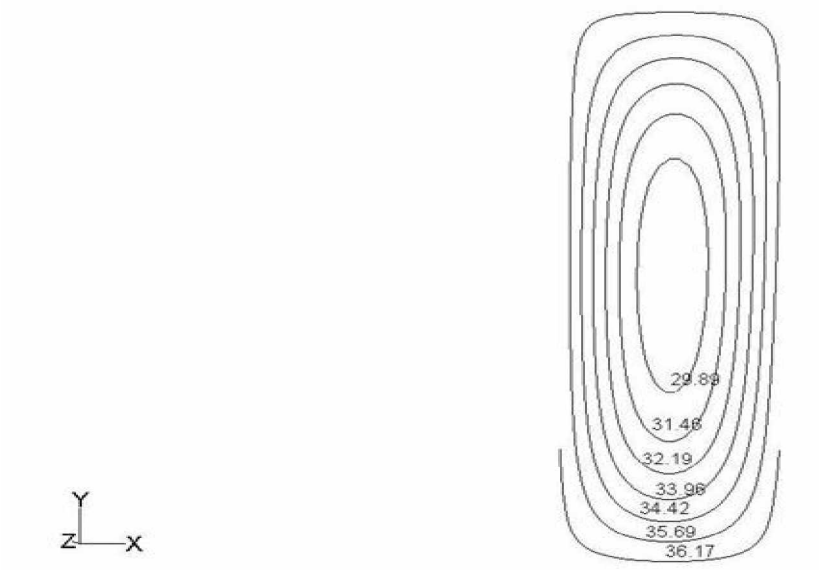

Fig (4.8): Temperature contour of fluid at outlet for Pressure difference of 50kpa and heat flux of 50W/cm^2 at X=50µm

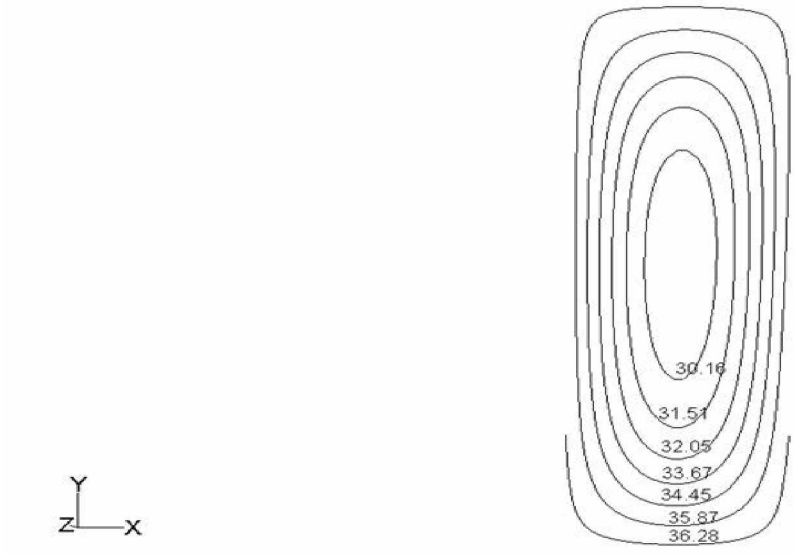

Fig (4.9): Temperature contour of fluid at outlet for Pressure difference of 50kpa and heat flux of 90W/cm^2

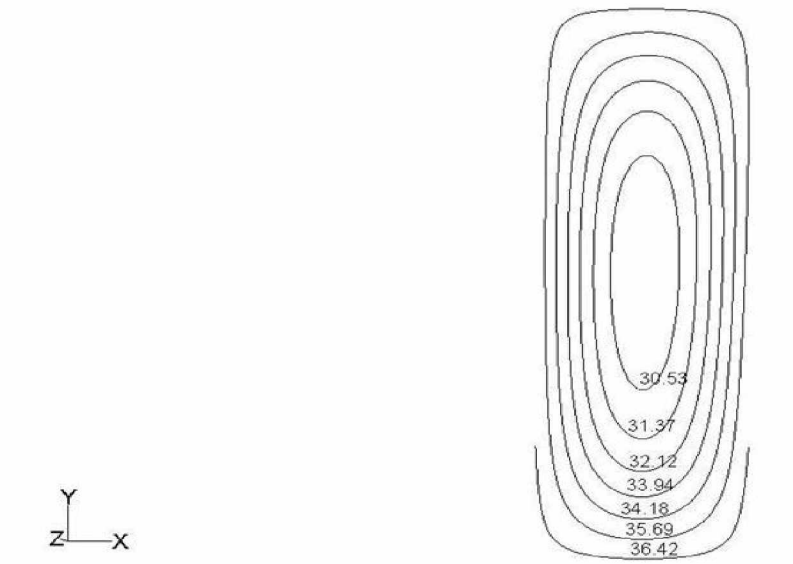

Fig (4.10):- Temperature contour of fluid at outlet for Pressure difference of 50kpa and heat flux of 150W/cm^2

In the current investigation, three different cases ($q"$ = 90 W/cm^2, Δp = 50kpa, 15kpa and 10 kpa) were considered here and local temperature distribution along the channel length was shown in Fig (4.11).Here the maximum temperature rise in case of 10kpa because the flow of fluid is very slow so fluid get sufficient time to heat up.

Fig (4.8), Fig (4.9) and Fig (4.10) displays the filled contours of temperature at outlet of the micro-channel for heat fluxes of 50 W/cm^2, 90 W/cm^2 and 150 W/cm^2 at a pressure difference of 50 kpa. As the heat flux increases, the outlet temperature goes on increasing because the fluid gets heated up more and more due to convective heat transfer which is evident from the contour profiles

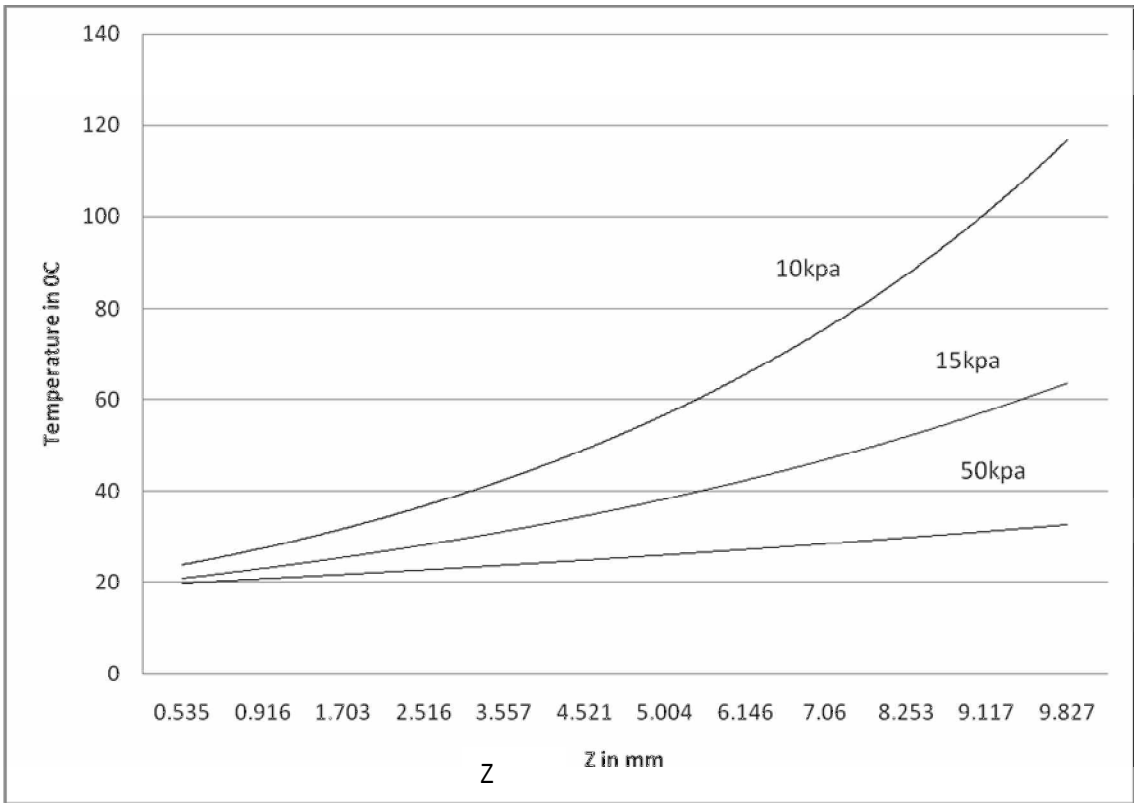

Fig (4.11):- Average temperature of liquid for different pressure drops and constant heat flux 90W/cm^2 at X = 50µm

Fig (4.11) and Fig (4. 12) displays the temperature at outlet of the micro-channel for heat fluxes of 50, 90 and 150 W/cm^2 at a pressure difference of 50 kpa. As the heat flux increases, the outlet temperature goes on increasing because the fluid gets heated up more and more due to convective heat transfer which is evident from the contour profiles..

$$T_{150} > T_{90} > T_{50} \qquad \text{(At 50 kpa)}$$

4.4 Velocity contour

Velocity contour at outlet of channel for pressure difference of 50kpa and heat flux of 90 W/cm^2 shown in Fig (4.12)

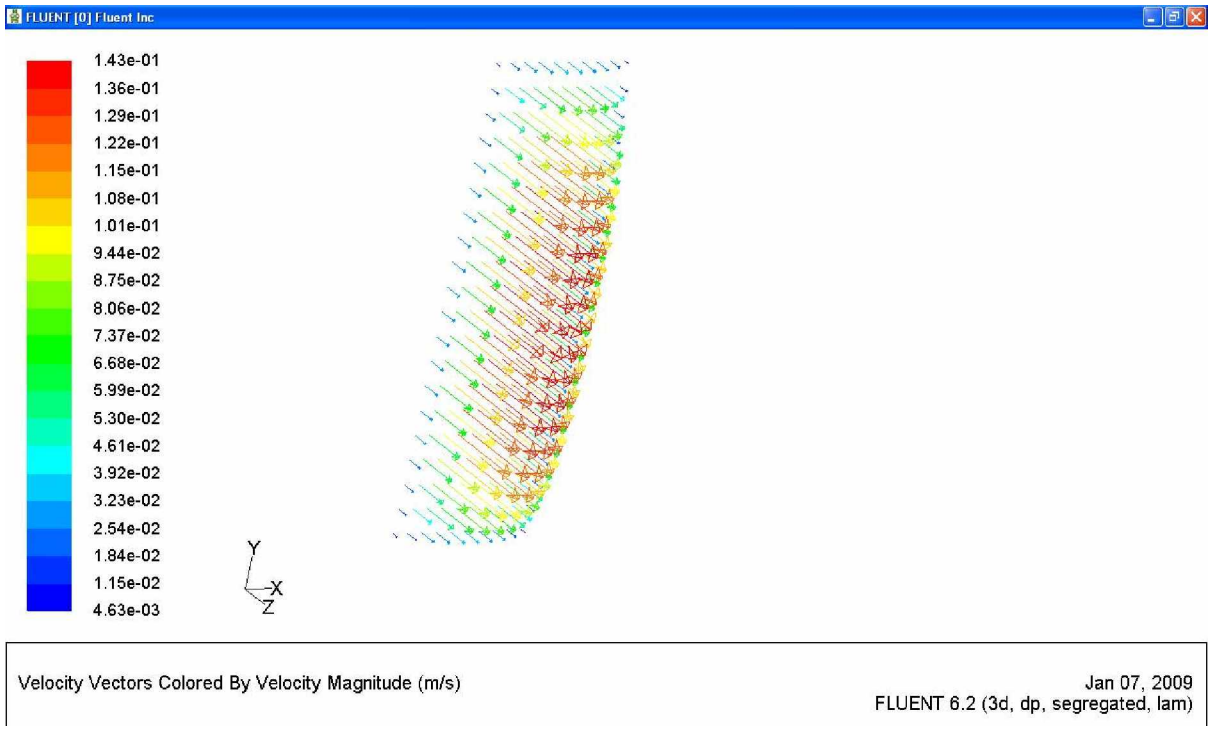

Fig (4.12) Velocity contour at outlet of channel for pressure difference of 50 kpa and heat flux of 90 W/cm^2

4.5.Average heat transfer coefficient

The variation of heat transfer coefficient is shown in Fig (4.13). It is found that the heat transfer coefficient sharply decreases at 1/10th of micro-channel. For this the temperature is also found less at the entrance region of water. The average heat transfer coefficient is simply defined as $h = \frac{q''}{\Delta T_{avg}}$, which is determined based upon the heat flux density applied to the bottom of the substrate and the temperature difference between the average substrate wall temperature and the bulk liquid temperature $\left(\Delta T_{avg} = T_w - T_l\right)$.

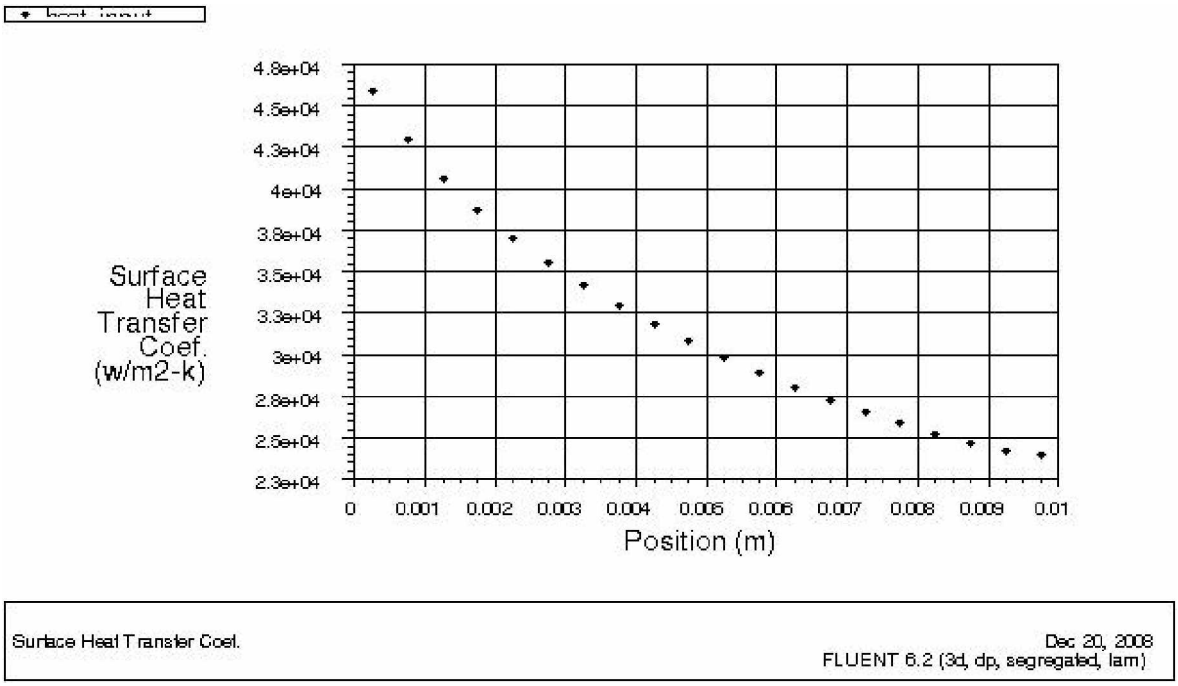

Fig (4.13) average heat transfer coefficient variation along channel for for Pressure difference of 50kpa and heat flux of 90W/cm^2

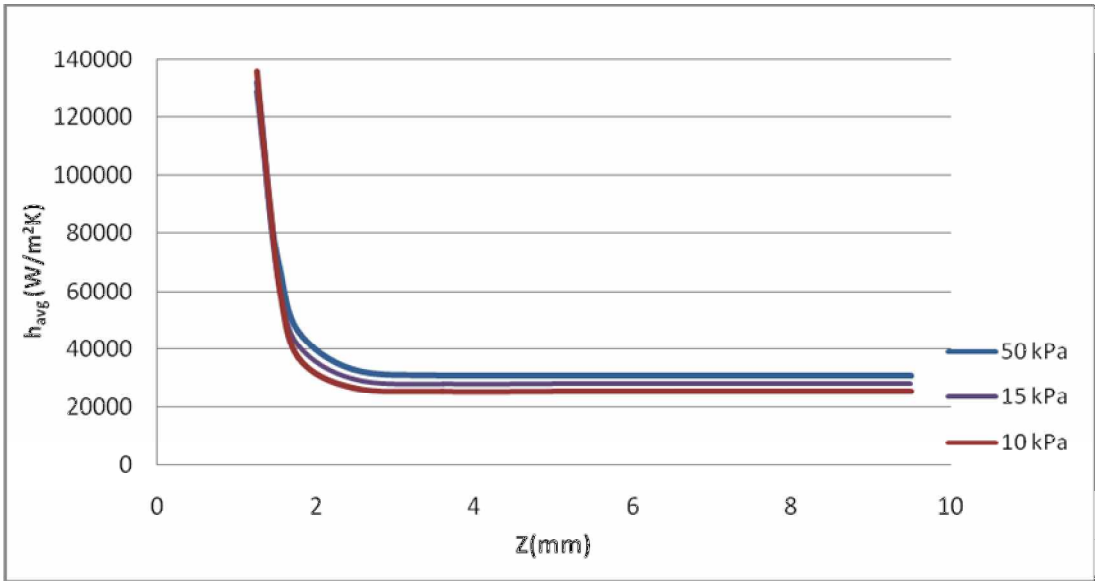

Fig (4.14):-Average heat transfer coefficient variation for different pressure drop (50kpa, 15kpa, 10kpa) at $q"= 90$ W/cm^2 at x = 50µm

4.6 Average Nusselt Number

Here we plot the average heat transfer variation for different pressure drops (50kpa, 15kpa, 10kpa) in Fig (4.14).It is justify by results here that the average Nusselt number 4.1 obtained here lies between the values for a constant axial wall heat flux, 4.8, and a constant axial wall temperature, 4.0, for fully developed laminar flow in ducts, of rectangular cross-section with approximately [W: H = 1: 3 (57:180)].

It is clear that if the definitions for the heat transfer coefficient and Nusselt number are used; the heat transfer will be underestimated at the entrance portion of the channel (especially close to the inlet) and overestimated towards the end of the channel. Here we do not consider either the heat conduction in the substrate and the conjugate heat transfer influence on the local heat flux variation along the longitudinal direction.

The average Nusselt number should be approximately 4.0 because of the limitations in the grid size used in the simulation developed here. The average Nusselt number is simply defined as $\frac{h.D_h}{k}$.

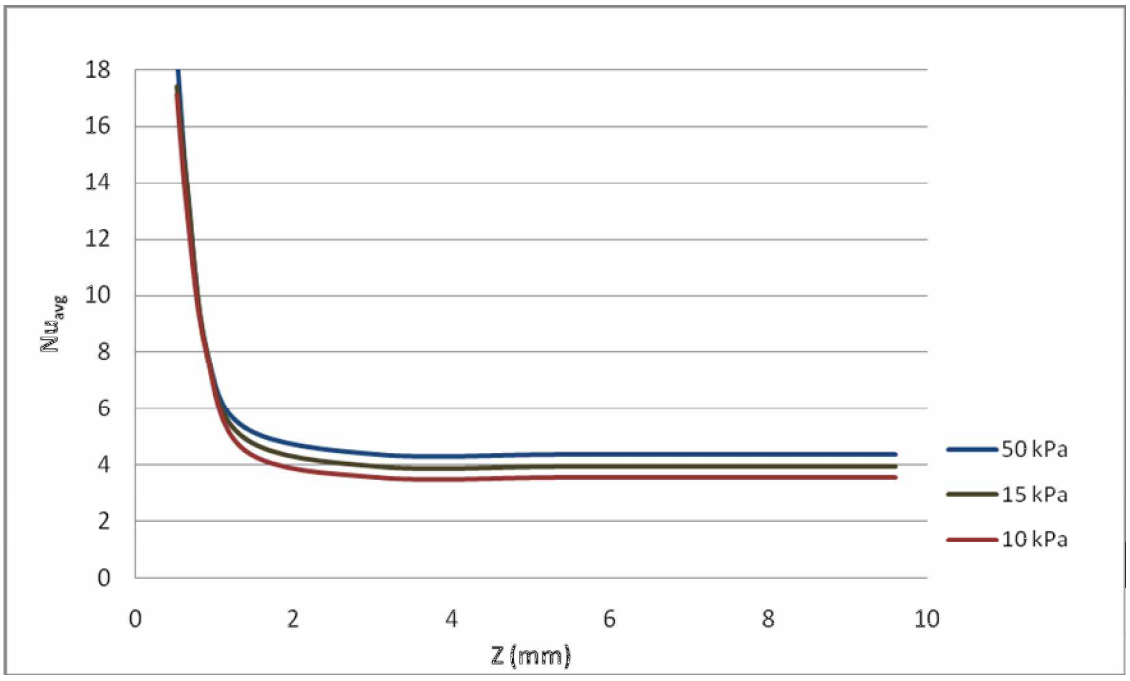

Fig (4.15):- Average Nusselt number variation for different pressure drop at 90 W/cm^2 at x = 50µm

The average heat transfer coefficient variation and the average Nusselt number variation for these three cases can be determined and are shown in (4.15) .The natures of output results are comparable with conventional results. From these two figures it can be concluded that the variations of the heat transfer coefficient and the Nusselt number along the flow direction is quite small for this type of microchannel heat sink after the thermal entrance lengths. It should be noted that since the grid size in the flow direction is relatively coarse, the local heat transfer is not as accurate or detailed as the case for the y- and x-direction. However the resolution is sufficient to aid in the design of micro heat sinks for industrial applications and also to provide information and insight in to the fluid flow characteristics in the flow direction.

Here we plot the average heat transfer coefficient variation along the channel length for different heat flux of magnitude 50W/cm^2, 90W/cm^2 and 150W/cm^2 in Fig (4.16).

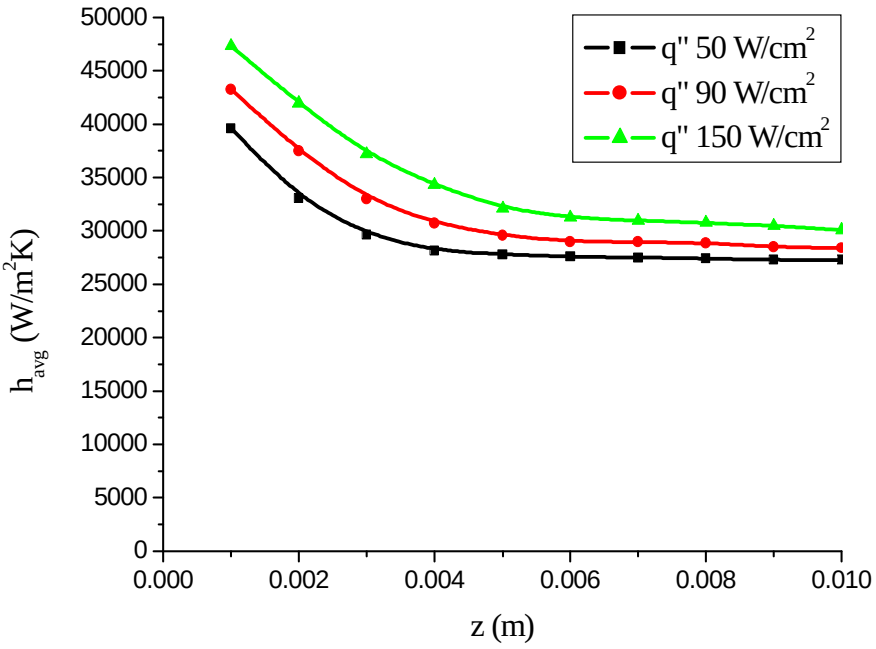

Fig (4.16):- Axial variation of average heat transfer coefficient for different heat fluxes at Δp = 50kpa

4.7 Nusselt number variation for different heat flux

Here we plot the Nusselt no variation along the channel length for different heat flux of magnitude 50W/cm^2, 90W/cm^2 and 150W/cm^2 in Fig (4.17).

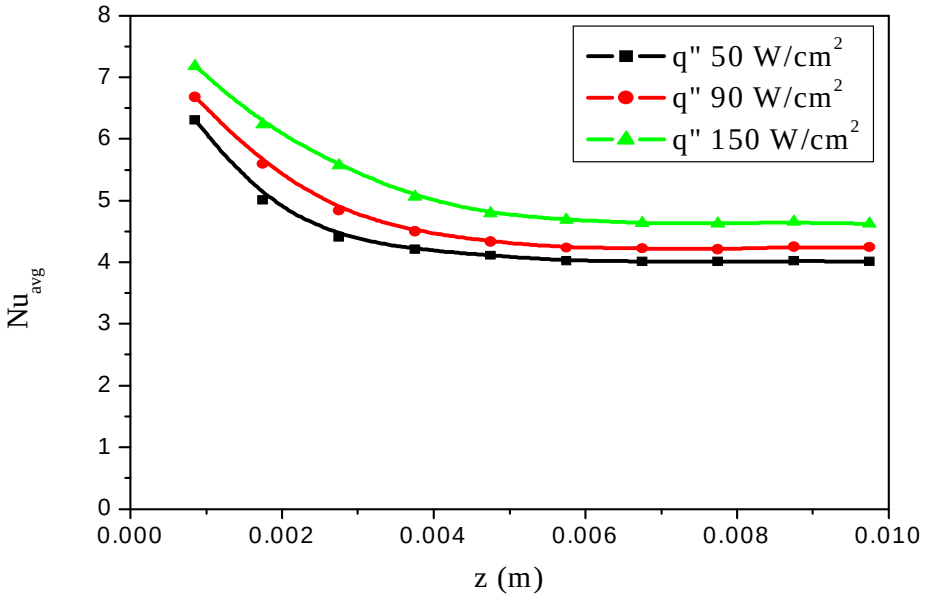

Fig (4.17):-Axial variation of Nusselt number for different heat fluxes at $\Delta p = 50$kpa

4.8 Reynolds number verses Nusselt Number

The average Nusselt number corresponding to their Reynolds number for different pressure drop at constant heat flux are plotted in Fig (4.18). In order to compare the experimental results with the simulation results, we considered different Prandtl number of water for different Reynolds number. Comparisons between the simulated results and the experimental results are plotted in Fig (4.19). The error is estimated to be 3% which is less than 5% so acceptable.

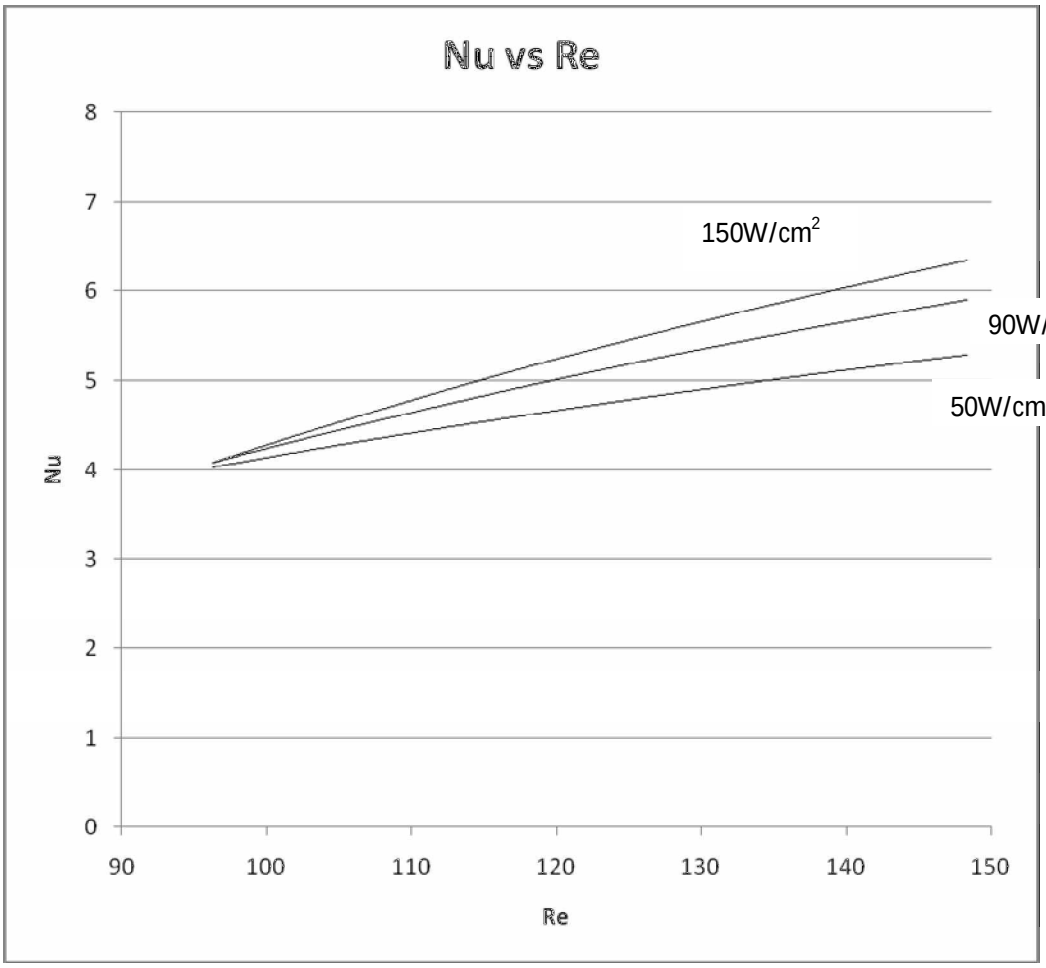

Fig (4.18):- Comparison between Nusselt number vs Reynolds number for Δp= 50kpa and different heat flux of 50 W/cm^2,90 W/cm^2,150W/cm^2

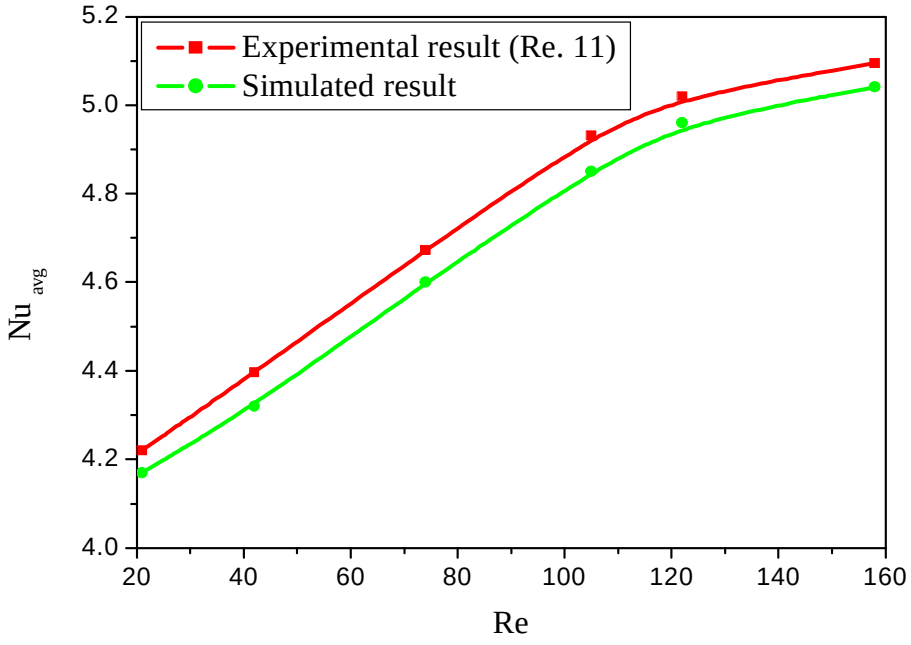

Fig (4.19):- Variation of Reynolds no vs Nusselt no in experimental work and simulated work

4.9 CONCLUSION

The analysis performed, provides a fundamental understanding of the combined flow and conjugate convection–conduction heat transfer in the three-dimensional micro-channel heat sink. The model formulation is general and only a few simplifying assumptions are made. Therefore, the results of the analysis as well as the conclusions can be considered as quite general and applicable to any three-dimensional conjugate heat transfer problems.

4.9.1 A three-dimensional mathematical model, developed using incompressible laminar Navier–Stokes equations of motion, is capable of predicting correctly the flow and conjugate heat transfer in the micro-channel heat sink. It has been validated using experimental data

reported in the literature, and a good agreement has been found between the model predictions and measurements.

4.9.2 The combined convection–conduction heat transfer in the micro-channel produces very complex three-dimensional heat flow pattern with large, longitudinal, upstream directed heat recirculation zones in the highly conducting silicon substrate where the fluid and solid are in direct contact. Here we have compare of the numerical results with other published results and experimental data available in the literature for Reynolds numbers less than 200 based on a hydraulic diameter of Dh = 86 μm. The influence of the geometric parameters of the channel and the thermophysical properties of the fluid on the flow and the heat transfer, are investigated with a temperature dependent thermophysical property. A correlation for the averaged Nusselt number with the Reynolds number is developed and discussed. The results indicate that variations in the way the Nusselt number is defined in different conditions.

4.9.3 As with the increase in pressure drop ,flow velocity as well as Reynolds number increase hence Nusselt number increases in consistence with Reynolds number analogy.

4.9.4 The local heat fluxes from the solid to the coolant in the small inlet region of the micro-channel are larger than those in the further downstream portion by more than two orders of magnitude. This is because the average convective heat transfer coefficient is much larger in the upstream locations (the boundary layer thickness is small) and also because the highly conducting channel walls support very effective heat redistribution from the downstream (large convective resistance) to the upstream (small convective resistance) regions of the channel. This finding supports the concept of the manifold micro-channel (MMC) heat sink where the flow length is greatly reduced to small fraction of the total length of the heat sink by using a design with multiple inter-connected inlets and outlets.

4.9.5 The result shows average Nusselt number increases with increase in pressure drop as well as heat flux.

4.10 Sources of Errors in CFD Calculations

The major source of error for a CFD analysis is due to the selected numerical method to solve Navier-Stokes equations. Some of the numerical techniques employed in CFD are Finite Difference Methods, Finite Element Methods and Finite Volume Methods. The one FLUENT uses is the Finite Volume Method and the source of error here arises when discretizing the transport equations. Interpolations are made to find values at the cell faces, whereas all the information is stored at the cell centers. This is the main approximation of the Finite Volume Method. Second type of error is at the Boundary Condition definitions. It is up to the user how to define the boundary conditions, therefore the results will be as correct as the user defines them.

All iterative solvers should run long enough to minimize the numerical error. Solver can be terminated at any time but great attention must be taken for achieving converged results. Default convergence criteria or predefined tolerances do not always assure converged results. One more important aspect to reduce the error in CFD calculations is to have a grid-independent solution. Grid must be fine enough to capture all flow features and analysis results must not change when the models are run with finer meshes. If the results are changing as the number of cells used are increased, then finer mesh should be created for grid-independency

4.11 Closure

An investigation of the fluid flow and heat transfer phenomena in microchannels and microchannel heat exchangers was conducted. A review of the literature published on research conducted in microchannel fluid flow and heat transfer over the two decades was completed. An analysis of some of the methods of experimentation and data reduction found in the literature was performed, and it was found that Major obstacles in implementing this technology are due to the lack of substantial understanding in the behavior of micro channel system. In reality, because it is difficult to achieve an adiabatic boundary at the inlet and outlet of the heat sink as assumed in the numerical model, a significant portion of the heat loss is transferred to the ambient environment, especially for low Fluid flow conditions.. .

A CFD model was created in Fluent to model the microchannels. The transition/turbulent Nusselt numbers from the microchannel model were corrected for

surface roughness effects and showed reasonable agreement with the magnitude and trend of the experimental turbulent Nusselt numbers.

For future work in the experimentation of MHE's, it is suggested that temperature measurements be made closer to the microchannel inlets and that temperatures be measured at more locations in the solid surrounding the microchannels and at near to surface where complex boundary layer is formed to obtain a better sense of how the heat flows through the entire MHE. Also, providing a higher wall temperature and/or lower inlet temperature would decrease the experimental errors that are incurred from the temperature measurements.

There is still a considerable amount of work to be done with the experimentation of microchannels and MHE's, and the prospect of the use of MHE's in high performance heat transfer applications looks more promising than ever.

BIBLIOGRAPHY

1. Tuckerman, D.B. and Pease, R.F.W., High-performance heat sinking for VLSI, IEEE Electron Device Letters, 1981

2. Wu, P. and Little, W.A., Measurement of friction factors for the flow of gases in very fine channels used for microminiature Joule-Thomson refrigerators, Cryogenics

3. Peng, X.F., Peterson, G.P., and Wang B.X., Heat transfer characteristics of water flowing through microchannels, Experimental Heat Transfer, 1994

4. Peng, X.F. and Peterson, G.P., Effect of thermofluid and geometrical parameters on convection of liquids through rectangular microchannels, International Journal of Heat and Mass Transfer, 1995, Vol. 38(4),

5. Judy, J., Maynes, D., and Webb, B.W., Characterization of frictional pressure drop for liquid flows through microchannels, International Journal of Heat and Mass Transfer, 2002

6. Liu, D. and Garimella, S.V., Investigation of liquid flow in microchannels, AIAA Journal of Thermophysics and Heat Transfer, 2004, Vol. 18, p. 65–72

7. Choi, S.B., Barron, R.F., and Warrington, R.O., Fluid flow and heat transfer in microtubes, Micromechanical Sensors, Actuators, and Systems, ASME DSC, 1991, Vol. 32, p. 123–134

8. Rahman, m.m.and gui. Experimaental measurements of fluid flow and heat transfer in microscale cooling passage in a chip susstrate.

9. Judy and Maynes, Three-dimensional conjugate heat transfer in the microchannel heat sink for electronic packaging, Int. J. Heat Mass Transfer 43 (3) (2000)

10. Lie and Garimella. Rectangular microchannels of different aspect ratios, International Journal of Heat and Mass Transfer 49 (2003)

11. Choi and Barron, Thermally developing flow and heat transfer in rectangular microchannels of different aspect ratios, International Journal of Heat and Mass Transfer 49 (2006) 3060–3067

12. Rahman and Fedorov ,Numerical Heat Transfer and Fluid Flow

13. Computational fluid Dynamics by Le.

14. J. Li and G.P. Peterson, Experimental measurements of fluid flow and heat transfer in microchannel cooling passages in a chip substrate, Proceedings of the ASME International Electronics Packaging Conference in Binghamton, NY, USA, ASME publications, 1993, Vol. 4-2, p. 685–692.

15 . Rahman, Vafai ,M.M. and Gui, F., Design, fabrication, and testing of microchannel heat sinks for aircraft avionics cooling, Proceedings of the Intersociety Energy Conversion Engineering Conference, 1993, Vol. 1, p. 1–6.

16 . `Wei and Joshi ,Enhanced heat transfer in the entrance region of microchannels, Proceedings of the Intersociety Energy Conversion Engineering Conference, 1995, p. 289–294.

17. Gui and Anderson, ., Single-phase liquid friction factors in microchannels, International Journal of Thermal Sciences

18 . Davies An experimental study of convective heat transfer in silicon microchannels with different surface conditions, International Journal of Heat and Mass Transfer, 2003

19 . Pucha, X.F., Wang, B.X., Peterson, G.P., and Ma, H.B., Experimental investigation of heat transfer in flat plates with rectangular microchannels, International Journal of Heat and Mass Transfer, 1995, Vol. 38(1), p. 127–137.

20. Zhao, X.F. and Peterson, G.P., Effect of thermofluid and geometrical parameters on convection of liquids through rectangular microchannels, International

Journal of Heat and Mass Transfer, 1995, Vol. 38(4), p. 755–758.

21 . Steinke, chen and Kandlikar, S.G., Single-phase liquid friction factors in microchannels, International Journal of Thermal Sciences, 2006, Vol. 45, p. 1073-1083.

22. Bau, P. and Weisberg , W.A., Measurement of friction factors for the flow of gases in very fine channels used for microminiature Joule-Thomson refrigerators, Cryogenics, 1983, Vol. 23(5), p. 273–277.

23 . Yin and Bau , Frictional flow characteristics of water flowing through microchannels, Experimental Heat Transfer, 1994, Vol. 7, p. 249–264.

24. Fedorov and Visakanta ,Heat transfer characteristics of water flowing through microchannels, Experimental Heat Transfer, 1994, Vol. 7, p. 265–283.

25. Zhao,X.F. and Peterson, G.P., Convective heat transfer and flow friction for water flow in microchannel structures, International Journal of Heat and Mass Transfer, 1996, Vol. 39(12), p. 2599–2608.

26. Pfund, D., Rector, D., Shekarriz, A., Popescu, A., and Welty, J., Pressure drop measurements in a microchannel, AIChE Journal, 2000, Vol. 46(8), p. 1496–1507.

27. Masud and Olsen, M.G., Aspect ratio effects on turbulent and transitional flow in rectangular microchannels as measured with microPIV, Journal of Fluids Engineering, 2006, Vol.128, p. 305-315.

28. Dhiman and A.K ., and Choi, W.K., Experimental investigation of flow friction for liquid flow in microchannels, International Communications in Heat and MassTransfer, 2000, Vol. 27, p. 1165–1176.

29 . Judy, Cheng ,Yal , Maynes, D., and Webb, B.W., Characterization of frictional pressure drop for liquid flows through microchannels, International Journal of Heat and

Mass Transfer, 2002, Vol.45(17), p. 3477–3489.

30. Kumara and Setal, Investigation of liquid flow in microchannels, AIAA Journal of Thermophysics and Heat Transfer, 2004, Vol. 18, p. 65–72.

31. Roy and Aet, Experimental and numerical study of pressure drop and heat transfer in a single-phase microchannel heat sink, International Journal of Heat and Mass Transfer, 2002, Vol. 45, p. 2549–2565.

32. Rodgers, An experimental study of convective heat transfer in silicon microchannels with different surface conditions, International Journal of Heat and Mass Transfer, 2003, 46(14), p. 2547–2556.

33. Wu, H. Weilin Qu, Friction factors in smooth trapezoidal silicon microchannels with different aspect ratios, International Journal of Heat and Mass Transfer, 2003, 46(14), p.2519–2525.

34 . Kohl, Ryu., Abdel-Khalik, S.I., Jeter, S.M., and Sadowski, D.L., An experimental investigation of microchannel flow with internal pressure measurements, International Journal of Heat and Mass Transfer, 2005, Vol. 48, p. 1518-1533.

35. Hetsroni, R., Laser, D., Zhou, P., Asheghi, M., Devasenathipathy, S., Kenny, T., Santiago, J., and Goodson, K., Experimental investigation of flow transition in microchannels using μm-resolution particle image velocimetry, Thermomechanical Phenomena in Electronic Systems Proceedings of the Intersociety Conference, 2000, Vol. 2, p. 148–153.

36. Lee, S.Y., Wereley, Hetsroni, Gui, L., Qu, W., and Mudawar, I., Microchannel flow measurement using micro particle image velocimetry, American Society of Mechanical Engineers Fluids Engineering Division Publication FED, 2002, Vol. 258, pp. 493–500.

37. Kambiz, K.V., and Adrian, R.J., Transition from laminar to turbulent flow in liquid filled microtubes, Experiments in Fluids, 2004, Vol. 36, p. 741–747.

38. Lior, H., Ewoldt, R., and Olsen, M.G., Turbulent and transitional velocity measurements in a rectangular microchannel using microscopic particle image velocimetry, Experimental Thermal and Fluid Science, 2005, Vol. 29, p. 435–446.

39. Li, Ewoldt, M., Micro PIV measurements of turbulent flow in square microchannels with hydraulic diameters from 200 m to 640 m, International Journal of Heat and Fluid Flow, 2006, Vol. 27, p. 123–134.

40 . Mala and Yoo, M., Flow characteristics of water in microtubes, International Journal of Heat and Fluid Flow, 1999, Vol. 20, p. 142–148.

41 . Tae hoji, Z.Y. and Li, Z.X., Size effect on microscale single-phase flow and heat transfer, International Journal of Heat and Mass Transfer, 2003, Vol. 46, p. 149–159.

42. Rheeetal and Hrnjak, P., Experimental investigation of single-phase flow pressure drop through rectangular microchannels, International Conference on Microchannels and Minichannels, ASME Publications, 2003, Vol. 1, no. 1028, p. 257–267.

43. De and Voe, Fluid flow and heat transfer in microchannels with rectangular cross section, Heat and Mass Transfer, 2007, http://www.springerlink.com/ (accessed May 2, 2008).

44. Fahler, M.J., and Gerner, F.M., Developing convective heat transfer in deep rectangular microchannels, International Journal of Heat and Fluid Flow, 1999, Vol. 20, p. 149-157.